THE EVERSHED EFFECT IN SUNSPOTS

by

ARVIND BHATNAGAR

A thesis submitted to the
Agra University

for the degree of

Doctor of Philosophy

Kodaikanal Observatory
Kodaikanal

July 1964

Certificate from the Supervisor

I certify that the thesis entitled "THE [illegible]" by Arvind Bhatnagar embodies the work of the candidate himself at the Kodaikanal Observatory. The candidate has worked on this thesis under my supervision for a period of nearly 2½ years. His attendance at Kodaikanal Observatory exceeds the prescribed minimum of 200 days.

M K Vainu Bappu

July 20 1964.

(M.K. Vainu Bappu)
Director
Kodaikanal Observatory

ACKNOWLEDGEMENTS

The present thesis is the result of work done during my stay at the Kodaikanal Observatory, as a senior research fellow from 1961 to 1964. I wish to thank the Ministry of Education of the Government of India for financial support during this period.

I feel greatly indebted to Dr. M.K. Vainu Bappu, who is responsible for suggesting this project. He has been extremely kind to provide me with all possible facilities required for this work. The untiring attention and inspiration he gave me, cannot be described in words. It is only Dr. Bappu's constant supervision, advice and sincere interest that made the completion of this thesis possible.

I am also greatly obliged to my colleague, Miss Nirupama Subrahmanyam. Her unceasing help, suggestions, and friendly discussions, were extremely useful in developing several ideas during all phases of the thesis. Miss Subrahmanyam's help in some of my computations is also thankfully acknowledged.

My special thanks go to Mrs. Yemuna Bappu for her constant encouragement and inspiration, which made my stay in Kodaikanal all the more congenial.

A word of thanks is too small a return for the help, encouragement and cooperation given by the entire staff of the Kodaikanal Observatory. It is difficult to name all the people who helped me in numerous ways. However, I would like to thank Mr. B.N. Bhargava, Dr. A.S. Ramanathan, Mr. J.V. Narayana, Mr. P.M. Nayar and Mr. A.P. Jayarajan for the keen interest that they have often displayed in my progress.

Mr. K.C.A. Raheem, ~~who~~, with his rich experience in instrument design, helped me a great deal. I am much obliged to him for his help.

I thank the workshop crew headed by Mr. L. Peter, for helping me in workshop jobs and for completing the modification of the Solar tower telescope dome etc., before the winter observing season of 1962-63.

The credit for many of the diagrams in this thesis goes to Mr. P. Shahul Hameed, who was kind enough to spend long hours in the darkroom making these photographs. Mr. M. Jan also helped him. My thanks are due to both of them. Mr. T. Mark assisted me a great deal at the telescope. I also wish to acknowledge the help rendered by Mr. C.G. Veeraraghavan.

Messrs R.K. Premakrishnan, K.K. Scaria, K. Rajagopalan and P.S. Abdul Kadir helped me in some of my calculations. I am grateful to these persons for their valuable help.

I would like to express my gratitude to the Director General of Observatories, India Meteorological Department for the privilege of working at the Kodaikanal Observatory.

I wish to express my appreciation for the assistance rendered by the staff of the computing section of the Physical Research Laboratory, Ahmedabad, in writing the IBM 1620 computer programmes necessary for reduction of the data.

Last but not ~~the~~ least, I am most grateful to Mr. S. Guruswamy for the painstaking job of typing this thesis.

TABLE OF CONTENTS

TABLE OF CONTENTS

SUMMARY

In the present thesis I have presented a detailed observational study of the Evershed Effect and associated phenomena in sunspots. The investigation was carried out at the Kodaikanal Observatory with the Solar tower telescope, yielding an image scale of 5".5 of arc per mm in conjunction with a 18-metre focal length Littrow spectrograph.

In chapter I, I have given a resume of the work done earlier on the Evershed Effect and an outline of the present investigation. I have emphasized that the influence of Zeeman broadening due to the sunspot magnetic field may obliterate the small scale velocity fields. To completely remove the effect of sunspot magnetic field, I have selected three Zeeman insensitive lines; 4912.027 A of Ni I, 5576.101 A of Fe I and 5691.508 A of Fe I (Ni), for velocity field determinations in sunspots.

In chapter II, I have described the instrumental arrangement and the observing technique for obtaining the spatial velocity field configuration. For a precise determination of small scale Doppler displacements in lines, large spectrographic dispersion and resolution are essential. For obtaining velocity field configurations, I utilized the fourth and fifth orders of the 18-metre spectrograph, with dispersions of 6 mm per A and 8 mm per A respectively.

On a high dispersion solar spectrum, of the kind used in this study, it is very difficult to measure precisely the small Doppler displacements. For measuring small Doppler shifts, I utilized a modified version of Evershed's positive-on-negative

method, using the principle of photographic subtraction. This modified positive-on-negative method, enables one to precisely and conveniently determine small Doppler displacements of the order of 50 metre per sec. The essential advantage of this method is that it is independent of the width of lines. The technique is described in chapter II.

I have also given in this chapter, the spatial distribution of the sight-line velocities obtained by using the earlier mentioned three Zeeman insensitive lines. Variations in the magnitude of velocity vectors in the three lines for the same disk position of the spot are an indication of the depth dependence of the velocity field in spot penumbrae.

To investigate changes in the velocity field pattern with the age of the spot, I carried out this investigation during two successive passages across the disk of the same sunspot group. I obtained spot spectra of Kodaikanal spot No.12368 for velocity field determinations before and after a rapid development of the spot group, which occurred during January 14 and January 18, 1963. I obtained 167 spectra using 3 lines for determining the spatial distribution of velocity fields in spots during the two passages. Sight-line velocities were determined at 3,340 points in the spots.

In chapter III, I have computed, using a recent sunspot penumbra model of Makita, the mean depths of formation of the two Zeeman insensitive lines 4912.027 A and 5691.508A. The three component velocities (radial, tangential and vertical) obtained from the measured sight-line velocities were computed, using an IBM 1620 computer and are given in this chapter. The radial

velocity pattern in sunspots, show a peak around half way across the penumbra. The magnitude of the peak velocity is a function of the line strength and of the disk position of the spot. At each of the nine disk positions of the spot, I obtained the gradient of the maximum radial velocity, U_{max} with depth. A mean gradient of U_{max} in the penumbrae was found to be 4.0×10^{-3} km/sec per km in depth. Small vertical velocities of the order of 0.3 km/sec and less, directed downwards in the spot penumbrae were also found.

My observations show the presence of sizable tangential velocities in the sunspot penumbrae. On six disk positions of spots, a slight systematic pattern in the variation of the tangential component could be seen. Maximum tangential components of the order of 0.6 km/sec were observed on six disk positions. When the spots are close to the centre of the disk, the tangential velocities show large variation in amplitude with no systematic pattern. The presence of this important tangential component is not confirmed fully. However, tangential velocities in spot penumbrae can be expected to exist, in the light of the recent measures of orientation and inclination of magnetic lines of force by Adam.

Also given in chapter III, is the spatial distribution of magnetic fields in spots for which velocity fields were determined.

In chapter IV, I have presented a photometric study of the phenomenon of asymmetry in lines, in the penumbral region. The credit for the discovery of this phenomenon also goes to Evershed. I have proposed a parameter called the 'Flag factor' (F.F.), as a measure of the asymmetry in lines. The variation of the 'Flag

factor', in and around the spot region and also with the disk position of the spots is given in this chapter. The asymmetry varies with the line strength and the magnitude of the maximum asymmetry decreases towards the disk centre positions of the spot. I have suggested that this phenomenon of asymmetry in lines may be due to the relative Doppler displacements occurring in several strata of the line forming layer.

Besides the large asymmetry in lines in the penumbral region, spectra obtained under almost superb atmospheric conditions show a diffuse wing in lines in the photospheric region. This phenomenon of diffuse wing in lines in the photospheric regions is more conspicuous in dark spaces between the bright solar granules. Lines acquire their normal shape in the brighter parts of the spectrum. This very interesting observation is reported in chapter IV.

Some of the finest spot spectrograms obtained under very good 'seeing' conditions (better than 1" of arc), show continuum brightness fluctuations in the penumbral region. A considerable variation in the width of the lines, along the length of the slit, in the penumbral region is observed. A correlation study between the continuum brightness, equivalent width and sight-line velocity is presented in chapter V. For this study three lines and three slit positions over the spot were used. The correlation study show that darker (cooler) regions of the penumbra show larger equivalent width, while the brighter (hotter) regions show smaller width.

I propose that these brightness fluctuations are the

manifestation of aggregates of small penumbral filaments, as seen on a good white light photograph of sunspots. The agency responsible for the widening of lines in penumbral region is more efficient in the darker interspaces compared to the brighter parts. It is believed that, this spectroscopic observation of brightness variations in the spot penumbral region is reported for the first time.

CHAPTER I

THE EVERSHED EFFECT IN SUNSPOTS

Evershed while analysing spot spectra taken at the Kodaikanal Observatory, for pressure determinations in sunspots, noticed that the spectral lines were displaced in the penumbral region. This displacement of lines in sunspot penumbrae was of a permanent character and persisted throughout the life of a spot. The magnitude of the displacement of lines varied with the disk position of the spot. Evershed (1909a) showed that the most favourable spot positions that show up the line displacement conspicuously were between 30° and 50° from the centre of the disk. Another interesting feature he observed, was that the magnitude of this displacement varied with orientation of the spectrograph slit. He found the displacement of lines to be a maximum, when the slit bisecting the spot was parallel to a line joining the spot and the centre of disk. In the slit position perpendicular to this direction, no displacements were observed. Evershed termed these two slit positions as radial and tangential respectively. Evershed also noticed that when the slit was parallel to the solar equator and crossing the spot centrally, the limb-side of the spot penumbra showed a displacement towards the red, while the centre-side exhibited a violet displacement. This was found to hold good for all disk positions of the spot.

All these observations convinced Evershed (1909a,b,c), that the displacement of lines was only due to the Doppler shift. This displacement was caused by the movement of the sunspot gases,

directed radially and horizontally outwards from the centre of the spot. The direction of motion of the sunspot gases, as found by Evershed was contrary to the velocity pattern expected on the basis of Hale's explanation of the likely origin of sunspot magnetic fields. Hale (1908) was led to believe from the appearance of H-alpha spectroheliograms that, the motion of sunspot gases was of a cyclonic nature, Hale argued that the solar corpuscles emitted by the sun are drawn into a cyclonic motion or a vortex and could give rise to a magnetic field in sunspots. Using the Zeeman effect, Hale was able to verify this conjecture by discovering strong magnetic fields in spots of the order of 2,000 to 3,000 gauss.

Evershed's early observations on the radial motion in sunspots were fully confirmed by the later observations of St. John (1913). This discovery of radial horizontal flow of material in sunspots, is now known in the literature as the EVERSHED EFFECT. The Evershed effect and Hale's discovery of magnetic fields in sunspots, created a bewildering array of difficulties for an appropriate theory of sunspots. Actually, we do not have to this day a good enough theory explaining all the observed phenomena concerning sunspots. It seems that the negative temperature gradient, strong magnetic fields and velocity fields in spots, have a strong interrelationship. A thorough investigation of all three of them may lead one to a possible coherent theory of the origin of sunspots. In this thesis we have concentrated on the aspect of velocity fields in sunspots. The spatial variations of magnetic fields in some of

the spots studied were also determined. Some of the requirements for such a study were fulfilled by the availability of a new solar tower telescope in conjunction with a high dispersion spectrograph the details of which are described in the next chapter. In the following we give a review of the work done on Evershed Effect.

Evershed (1910) extended the study of velocity fields in sunspots to investigate the variation of radial velocity with the strength of lines. He showed that the stronger lines indicate smaller velocities compared to those obtained from the fainter lines. Lines of Rowland intensity 0 to 1 give velocities of 2-3 km/sec., while lines of 5 to 6 Rowland intensity give 1.4 km/sec. Further, the radial velocity increases monotonically from the umbral boundary to become a maximum near the outer penumbral boundary. Evershed's measures of radial velocity refer to only the maximum values in the penumbra. In his earlier works, Evershed (1909a,b) maintained that the motion abruptly ceases near the periphery of the penumbra. But in his later studies (Evershed 1913) he has shown that the motion continues outside the spot also. The displaced lines regain their normal wavelength slowly at about 8,000 kms beyond the spot boundary. This has been confirmed by later workers, as well as by us and will be described in chapter III.

Besides the radial outflow of sunspot gases in the lower photospheric level Evershed (1910) investigated also the behaviour of the chromospheric gases over sunspots, using the central absorption lines of Ca^{+}. These chromospheric lines showed that the matter, instead of moving outwards was moving inwards towards the centre of the spot, showing an indraught of calcium vapour in the

higher chromosphere. The average radial velocity of these gases was found to be about 1.8 km/sec.

St. John (1913) at Mount Wilson followed the work of Evershed on the Evershed Effect, using instruments with larger spatial resolution and also higher spectrographic dispersion. It is indeed very surprising that, this very obvious radial motion of gases in spots escaped detection by the Mount Wilson Observers during their earlier studies of sunspot spectra. St. John (1913) used some 506 lines representing a large number of elements with a wide range in their line-intensities and excitation potentials, for velocity field determinations in spots. He also included some chromospheric lines and the very strong lines of Fe, Mg and Al. The method of observation was to juxtapose the spectra of the two sides of a spot side by side. Half the total displacement then gave the line of sight component of velocity. He obtained the mean radial velocity observed in eleven spots for each of the 506 lines. These eleven spots were randomly distributed over the disk and the mean umbral diameter was about 8,000 kms. He showed that for iron lines of Rowland intensity 0, the outward radial velocity was 2.04 km/sec. The velocity values become zero for Rowland intensity 15 and higher. But for stronger lines such as those of sodium D_1 and D_2, magnesium b and for stronger chromospheric lines, the direction of motion was opposite that is, inwards towards the centre of spot. The magnitude of the inward radial velocity also increases with increasing intensity of lines and becomes about 3.8 km/sec. for the lines of ionized calcium.

St. John (1913) assuming the hypothesis that fainter lines

are formed deeper while stronger lines are formed higher in the photosphere, gave a radial velocity field model with depth. According to this model the magnitude of the outward radial velocity in sunspots decreases with height in the photosphere, becomes zero near the reversing layer and then increases with sign changed with increasing height.

The radial velocity field model of St. John, fascinating as it is, requires serious consideration. Infact, it has become clear from Evershed's work that the lower sunspot gases are flowing outward, while the higher chromospheric gases inward, towards the spot centre. This would imply that there is a continuous outflow of material, perhaps from the umbra of the spot. The loss due to the outflow is perhaps replenished by fresh material from the chromosphere. To test this hypothesis, Evershed (1910) attempted to detect an ascending motion in the umbra, using the photospheric lines. But contrary to this, he found, if at all, a descending motion of the order of 0.4 Km/sec in spot umbrae. This observation complicates the concept of maintaining a balance between the outgoing and incoming material in spots. Where does the material giving rise to a continuous outflow in the lower layers originate from? Does the inward flow observed in the lines of chromospheric origin terminate in the umbrae and thus possibly replinish the loss experienced in the outflow in the photospheric levels? These are questions that have yet to find an answer.

Evershed's detailed study of about seventeen spots, clearly revealed a hirozontal radial outflow of material in sunspot

penumbra. To estimate further the contribution due to the tangential component of velocity, Evershed (1910, 1916) studied 5 spots with the slit placed tangential and crossing the spot. He detected a tangential (rotational) component of the order of 0.36 km/sec. and in some cases higher, near the outer boundary of the penumbra. The direction of rotation was counter-clockwise for some spots while clockwise for others. Compared to the tangential velocity, the mean radial velocity was found to be about 2 km/sec. The motions when coupled give a spiral wheel movement.

Much later Abetti (1932) observed 26 spots and reported that the radial velocity varies from 0 to 5.0 km/sec. and the tangential velocity also varied from 0 to 5 km/sec. from spot to spot. He showed that the radial velocity is a function of the spot area. Michard (1951) utilizing Abetti's data showed that the magnitude of radial velocity increases with both magnetic field and spot area. Another conclusion which Michard drew was that the maximum radial velocity is a function of the spot's position on the disk. At larger distances from the disk centre, that is near the limb, the radial velocity was found to be small compared to those found in spots located near the disk centre. This implies that near the limb, where one sees only the superficial layers of the solar atmosphere, the radial velocity in spots is small. This conclusion is in agreement with St. John's and Evershed's observations. Michard (1951) gives an empherical relation between the angle θ (angle subtended at the disk, between the line joining the observer and the direction normal to the solar surface), and the maximum radial velocity as follows:

$$v = v_0 (1 - 0.8 \sin \theta)$$

It was first realized by Evershed (1909d) that the magnitude of radial velocity varied in the penumbral region. He noted that the lines become convex or concave towards the general Evershed flow, when the slit is placed crossing only the penumbral regions. However, no serious attempt was made until Kinman (1952), who studied the aspect of spatial distribution of velocity field in sunspots. The details of image scale and dispersion used by Kinman are given in Table (I.1). Kinman (1952, 1953) obtained several spectra with the slit set at different positions over the spot. To determine the spatial velocity field in $\overset{o}{A}$spot, he measured the sight-line velocity along the length of the slit, in and around the spot. In his first study Kinman (1952) utilized some fifteen lines of Rowland intensity varying from 0 to 6. He obtained the mean sight-line velocity from the fifteen lines, at 237 points in the spot region. Working on the hypothesis that the flow of material in spots has a cylindrical symmetry about the spot centre, he obtained radial, tangential and vertical velocity components in spots.

The radial velocity pattern obtained by Kinman shows a peak around the middle of the penumbral region. The maximum radial velocity, U_{max}, was found to be a function of spots diameter (kinman 1953). For a spot umbral diameter of 12,000 kms, Kinman obtained U_{max} of the order of $\backsim$ 1.79 $\pm$0.13 km/sec. Kinman also discovered maximum tangential velocities of the order of about 0.5 km/sec., but he believes that these velocities were much less than their r.m.s. errors. A systematic vertical upward velocity of about -0.3 km/sec. was also found by him, but he assigned this to some systematic error in the measurements. From Kinman's

studies of Evershed Effect, it is well established that from its maximum value of about 2 km/sec, the radial velocity decreases to become zero far out in the photosphere. This is exactly what Evershed (1916) observed and is fully confirmed by many workers and by us. Recently Brekke and Per Maltby (1963) have repudiated this finding. They have shown from the observations of a single spot that the radial velocities abruptly cease at the outer boundary of the penumbra.

Kinman (1953) suggested that the measured sight-line velocities may be affected by the following obliterating influences;

1. the horizontal apparatus function of the spectrograph,

2. the Zeeman broadening,

3. obliteration of the solar image due to the telescope, spectrograph and atmospheric conditions, and

4. scattered light in the telescope and spectrograph etc. Kinman (1953) has given a method for evaluating the telescope scattered light. Using this method he finds that the scattered light in the Oxford telescope and spectrograph, can modify velocities by as much as 10 per cent in extreme cases. Recently, Holmes (1963) has shown that the influence of scattered light in velocity measures is more near the solar limb positions than near the disk centre.

Another very interesting phenomenon that accompanies the Evershed Effect, is the development of asymmetric wings in lines. The credit for the discovery of this phenomenon also goes to Evershed (1916). He observed considerable variation in the width of lines near the outer boundary of penumbrae, while the lines acquired their normal width in the photosphere. Evershed reports

about this phenomenon as, "....they (lines) are in some cases twice the normal width, with a tendency to diffuse in the direction of displacement, indicating velocities still higher than those measured for a portion of the absorbing gas". In Figure 2 of his paper (Evershed 1916), Evershed has clearly shown that lines develop a diffuse widening near the limits of penumbra. It is exactly this widening that we see easily on high dispersion sunspot spectra similar to those obtained by McMath et.al (1956).

Recently, Bumba (1960) at the Crimean Observatory has studied this phenomenon in great detail. He used large spectrographic dispersion and a large solar image, the details of which are given in Table (I-1). He reported that in the Evershed Effect, lines in the penumbra develop strong asymmetry, towards the general Evershed flow. He termed this asymmetry in spectral lines as 'Flag'. Under unusual atmospheric conditions, he claims to have resolved this 'flag' into a separate 'satellite line'. Servajean (1961), has also studied this phenomenon. It seems that Bumba (1960), Servajean (1961) and other workers in reporting the phenomenon of asymmetry in lines, seemed to have overlooked the pioneering discovery made by Evershed in 1915. We have attemptedto investigate photometrically, the variation of asymmetry with the disk positions of the spot, and also in and around the spot, This study is presented in Chapter IV.

Another investigation on the Evershed Effect was recently carried out by Servajean (1961). He used some 124 lines of Rowland intensity varying from 0 to 8, to determine the maximum radial velocity in one sunspot and at one disk position of the spot. From the theory of line formation for faint lines and using Michard's

TABLE I.1

Details of instrumentation used in the study of the Evershed Effect.

Author	Year	Dispersion A/mm	Doppler shift on plate mm/km/sec.	Image scale "of arc per mm	Exposure time in sec.	No.of spots studied.
		mm/A°				
Evershed	1909	1.1	0.014	16.3	30	12
Evershed	1909	1.1	0.014	16.3	30	4
Evershed	1916	1.1	0.014	22.0	5-30	2
St.John	1913	0.53 1.78	0.025	11,8	60-180	11
Abetti	1932	1.2	0.013	11.0	-	26
Calamai	1934	1.2	0.013	11.0	-	5
Kinman	1952	1.5	0.013	10.3	5-6	1
Kinman	1953	1.5	0.013	10.3	2-5	4
Bumba	1960	0.29 3.45	0.063	5.9	1-2	22
Servajean	1961	0.5 2.0	0.02	9.0	1-12	1
Holmes	1961	0.17 5.88	0.109	5.8	30-60	1
Holmes	1963	0.20 5.0	0.092	10.3	40-60	1
Bhatnagar	1963	0.12 8.33	0.137	5.5	10-12	2
		0.17 5.88	0.109	5.5	3	2
		0.167 5.99	0.113	5.5	3	2

(1953) model for the sunspot umbra, he determined the gradient of maximum radial velocity in the penumbral region. The maximum radial velocity variation found by Servajean is not linear with depth. The gradient for small values of τ = 0.01 (100 kms) is about 0.006 km/sec, per kilometre in depth; for τ = 0.03 (175 kms) the gradient is 0.003 km/sec, per kilometre, but for deeper layers τ = 0.07 ($\approx$ 300 kms) the velocity gradient is about 0.004 km/sec per kilometre. Besides this study, Servajean (1961) determined at six disk positions of a spot, the radial, tangential and vertical components of velocity. He made use of only one Zeeman insensitive line at 5691.508 A of FeNi for this study. From this investigation he concluded that the maximum radial velocity in spots increases with increasing values of μ (Cos θ), that is, higher layers of photosphere show less radial velocity in spots compared with the deeper ones. This conclusion of Servajean has been questioned by Holmes (1963). According to her the variation of the maximum radial velocity with disk positions, may not be wholly due to the level difference in the solar atmosphere, as interpreted by Servajean and earlier by Michard (1951). Holmes believes that the decrease of radial velocity towards the limb positions, may be due to the increasing scattered light contribution. This objection may be valid when one line is used for velocity measurements. Along with the large component of radial velocity, Servajean detected tangential and vertical velocities of small amplitude. He believes that the tangential component is erratic and hence can be neglected, but vertical velocities of amplitude 0.3 km/sec. directed inwards, show real motion of descent in penumbrae. Holmes (1961) reported a study of Evershed Effect,

in a single spot of about 12,000 kms umbral diameter. For simplifying the calculations, she neglected the tangential velocity and confirmed the earlier findings of Evershed and many other workers. To avoid the obliterating influence due to Zeeman broadening in spots, she used a Zeeman insensitive line of FeI at 5576.101A. Our results of these component velocities in spot penumbrae are given in Chapter III.

Recently, Schroter (1963) measured for the first time in integrated light, the movement of bright 'knots' in sunspot penumbra. He made use of the solar photographs taken by stratoscope I. These photographs show unusually fine details of the order of 1/3" of arc. Schroter observed that the bright 'knots' in the penumbral region show systematic outward motion of the order of 1 to 2 km/sec. This movement he interprets as the manifestation of the Evershed Effect in white light. Some of my plates taken with the 18-metre spectrograph under 'seeing' conditions where the tremor disk is less than 1" of arc, show continuum brightness fluctuations in the penumbral region. These brightness fluctuations, I believe are due to aggregates of 3 to 4 bright penumbral filaments. The brighter regions show systematically smaller sight-line velocities than the neighbouring dark spaces. Fluctuations in line width are also observed. A detailed study pertaining to the continuum brightness fluctuations in penumbral region is given in Chapter V.

From the above review of the earlier work done for the study of Evershed Effect, we see that this effect along with other associated phenomena requires high spectrographic dispersion, high spatial resolution of the solar image,and good atmospheric conditions.

In Table (I.1), we give briefly the details of dispersion, velocity factor, scale of solar image, number of spots studied, exposure time etc. used by earlier workers and by me, in the present investigation. The dispersion and image scale used in the present study are the highest utilized thus far. The seeing conditions, which is an equally important consideration, were very good during our observing spells. Spectra obtained under less than average seeing were discarded and not included in this study. The spot spectra taken in February 1963 and used in this study, show very fine details. These were obtained after a heavy spell of rains. It has been the experience at Kodaikanal that seeing and sky transparency becomes superb after a rainy spell. We noticed under very good seeing conditions (less than 1" to 1.5" of arc) that the visibility of solar details on the spectrograms, was not affected even when the exposure times were of 10 to 12 seconds duration. The high quality of the spectrograms can be judged by the appearance of 'streaks' in the continuum due to the solar granulation and also 'streaks' in the penumbral regions.

CHAPTER II

The observations

2.1. Experimental technique.

For a detailed and precise knowledge of the spatial velocity field distribution and other associated phenomena, it is essential to have high spatial resolution of the solar image and also, large spectrographic dispersion. Both these requirements were fulfilled by the availability of a solar tower telescope in conjunction with a high dispersion spectrograph. A 60.0 cms aperture coelostat and a 60.0 cms secondary mirror are mounted on top of a tower 9.2 metres in height. The light from the secondary is directed towards a third fused quartz flat of 60 cms aperture at the bottom of the tower from where it is directed horizontally to the telescope in an underground tunnel. This tunnel houses the 37.5 cms aperture solar telescope and the 18-metre spectrograph. The 37.5 cms lens is a two element achromat of focal length 36.6 metres and yields an image of the sun 34.8 cms in diameter. The image scale of the solar telescope is therefore 5.5 seconds of arc/mm. A schematic drawing of the optical train is given in Figure II.1. The spectrograph is of a Littrow type, using a two element achromat of 20.0 cms aperture and 18 metres focal length. A very fine grating ruled by Dr. Babcock is used as the dispersing unit. The grating of 600 grooves/mm is blazed in the fifth order green, and has a ruled surface of 200 x 135 mm. The theoretical resolving power of the Babcock grating is 600,000 in the fifth order. Tests performed with Iodine tube, have shown that close Iodine doublets at 5330 A

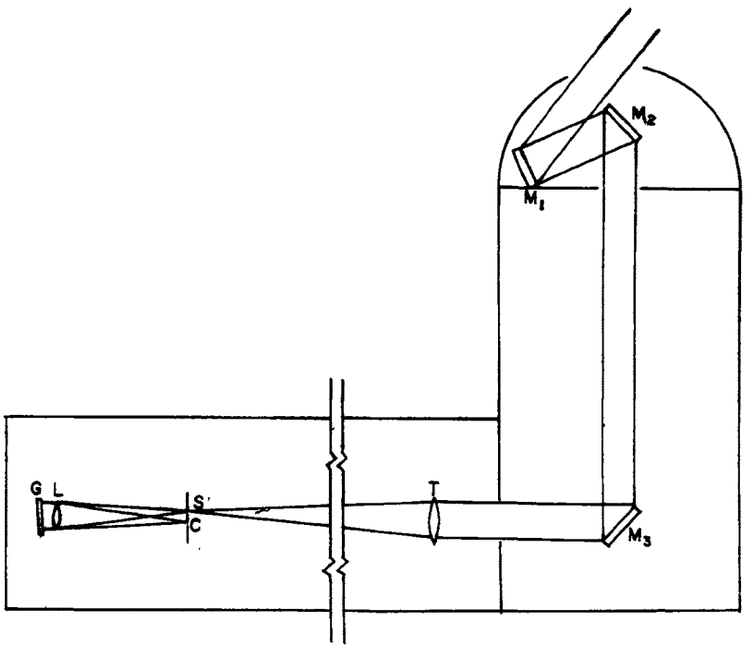

Figure II.1.- Schematic diagram of the optical system,
M_1: 60-cm Coelostat,
M_2: 60-cm secondary,
M_3: 60-cm lower mirror,
T: 37.5 cms aperture, 36-metre focal length objective
S: slit of the 18-metre spectrograph,
C: camera end,
L: 20-cm Littrow lens,
G: 200 x 135 mm Babcock grating.

region, having approximately 0.009 A separation can easily be resolved, in the fifth order. The grating thus yields theoretical performance in the fitth order. Dispersion obtained in different orders and wavelength regions, are given in Table II.1. The 18 metre Littrow spectrograph has a slit, 55 mms long. The spectrograph lens is mounted on a moving carriage and can be remotely moved by an electric motor. We determined the colour curve of this lens, using the iron arc as source.

The camera end can accommodate plates of 3" x 12" size. To obtain several spectra on the same 3" x 12" plate, we placed a diaphragm having a square aperture two inches on the side. The plate holder can be slid to bring different portions of the plate before the aperture, thus enabling one to obtain 6-spectra of the same spectral region in quick succession. This facility has been a great advantage for the spatial study of velocity and magnetic fields in sunspots.

To estimate the scattered light in the spectrograph, we performed a few tests. A couple of spectra were taken with the slit height varying from 0,5 cms to 2.5 cms. We gave long enough exposures to greatly over expose the spectra. No blackening beyond the spectrum edges on these exposures is perceptible. Photoelectric determinations of the diffuse scattered light in the spectrograph, have also shown that it is less than half a per cent. We therefore neglect the scattered light contribution to the measured velocities of spectrographic origin.

2.2. Observational technique.

To establish a complete velocity field around sunspots,

TABLE II.1

Dispersion on the plate in various orders

Region Å	Order I mm/A	II mm/A	III mm/A	IV mm/A	V mm/A	VI mm/A	VII mm/A
3950	1.0	2.1	3.4	4.9	6.8	9.4	13.8
4900	1.1	2.2	3.7	5.4	8.1		
5900	1.3	2.2	3.8	6.1	11.7		
6563	1.8	2.4	4.0	6.8			

we obtained several spectra with the slit crossing various portions of the spot. During our observing period the slit was approximately in the north-south direction. Generally, five to six slit positions were found enough to cover the whole region of the spot. In the spot penumbrae, both magnetic and velocity fields are observed. A precise determination of the velocity field is greatly facilitated if one can eliminate the interfering influence caused by the Zeeman effect. A symmetrically broadened line by the normal Zeeman effect may not affect the velocity measures. But due to any instrumental polarization a partial suppression of one of the σ - components can occur. The instrumental polarization exists definitely, since one uses a number of aluminized mirrors at different angles. To avoid completely the influence of the magnetic field, we select for velocity measures, three lines that are insensitive to the Zeeman effect. Details of these lines are given in Table II.2. The basis of selection was to include lines free of blending and which are representative of a range in intensity as well as excitation potential.

It is also important to know precisely the coordinates of the points where the displacements were measured on the spectrograms. To achieve this, the orientation of the slit and the disk position of the spot was precisely determined by the following method. Two thin wires of about 0.2 mm thickness, were stretched by springs over the slit jaws and separated by about 1.5 cms. These wires cast shadows on the spectrum and served as fiducial marks on the plate. The spot spectra were taken after bringing the desired portion of the spot between these two wires. A

TABLE II.2

Details of Zeeman insensitive lines used for velocity field measures

Wavelength Å	Element	Rowland Intensity Disk	Rowland Intensity Spot	E.P Lower	E.P High	R.M.T Multiplet No.	Multiplet
4912.027	Ni I	1	1	3.75	6.26	111	$z^5F^o - e^5F$
5576.101	Fe I	4	4	3.42	5.63	686	$z^5F^o - e^5D$
5691.509*	Fe I	2	2	4.28	6.45	1087	$y^5F^o - g^5D$

*This line is identified as blend of Fe (Ni) in Rowland's Table.

recording of the positions of the wires, the slit position and the spot is made, immediately on termination of the exposure. These sunspot maps with the wires and slit position marked, were later used during the measurement of the spectra. The coordinates of the points at which the velocity measures were made, were determined by using these sunspot maps and the white light photoheliograms taken daily at Kodaikanal around the time of the spot spectra exposures. The orientation of the slit with respect to the east-west line was determined by trailing the solar image across the slit. Coinciding the east-west line drawn on the 34.8 cms image with the enlarged copy of the photoheliogram of the same day, we determined the orientation of the wires, with respect to the true north of the sun. The position angle ϕ and the radial distance γ of these two wire locations were determined. Using the well known formulae, we calculated the heliographic latitude B and longitude L for the two wire positions. These were plotted on a graph paper with $X = (L-L_0)\ \mathrm{Cos}\ B$ and $Y = B$, where L_0 is the heliographic longitude of the sun's centre. A line joining these two points directly gives the slit position over the solar disk. From these plots one can easily determine the heliographic coordinates of any point over the slit. The advantage of this method is that, from a knowledge of the coordinates of two points over the disk, coordinates of all other points in the spot can be directly obtained. The only assumption we make is that the surface around the sunspot ($\approx$ 3 degrees) region is plane.

To avail all possible opportunities of sunspot availability

close to the minimum, and of weather, we obtained spot spectra of as many spots as possible. For the final analysis we left out spot spectra of 3 spots, as being less satisfactory for a precise velocity measurement. Our criteria for the selection of spot spectra were as follows:

1. the spectrum should be of good quality
2. the spot should be stable and symmetrical

and 3. the seeing during the exposures should be good.

In Kodaikanal, the best observing season falls during the December, January and February months. The seeing and transparency conditions usually show a marked improvement after spells of heavy rains. The observations incorporated in this study were made on 3 days in December 1962, 15 days in January and 15 days in February 1963. As many spectrograms as possible of the same spot, on different disk positions were obtained during its passage. For the velocity field studies we used only some of the spot spectra taken during January and February 1963. In Table II.3, we give the details of the spot spectra obtained with the 18-metre spectrograph and which are used in this thesis for a study of sunspot velocity fields. The spectra taken during the month of February 1963 were all calibrated for photometry. The calibration was effected on the same plate using an out of focus image of centre of the solar disk and a Hilger 6 step wedge. Some of the calibrated spectra were also used for a detailed photometric study of the lines. These measures are reported in Chapters IV and V.

All the plates were developed at 20°C in D-11 developer

TABLE II.3

Details of the spectrograms obtained for the study of Evershed Effects in sunspots

Plate No.		Exposure time in U.T h. m. s.	Duration of exposure in sec.	Region A	Order of grating	Seeing	Sky transparency in $10^{-6}\odot$
	Jan. 13, 1963 in spot No. KKL 12368 at μ= 0.77						
A153	a	06 03 55	7	5576	IV	2-3	
	b	06 06 00				2-3	
	c	06 09 55				2-3	
	d	06 24 25				2-3	
	e	06 25 30				2-3	
	f	06 28 01				2-3	
	Jan. 19, 1963 in spot No. KKL 12368 at μ= 0.75						
A172	a	02 05 10	7	4912	IV	3-4	48-52
	b	02 08 10				3-4	
	c	02 10 45				3-4	
	d	02 16 20				3-4	
	e	02 19 20				3-4	
A173	a	02 26 05	7	4912	IV	3-4	
	b	02 28 10				3-4	
	c	02 30 30				3-4	
	d	02 35 25				3-4	
	e	02 37 45				3-4	
	Jan. 20, 1963 in spot No. KKL 12368 at μ= 0.53						
A180	a	02 04 45	5	5691	IV	2	85-92
	b	02 07 20				2	
	c	02 09 30				2	
	d	02 11 50				2	
	e	02 14 25				2	
	f	02 16 30				2	
A181	a	02 26 55	5	5576	IV	2	
	b	02 28 40				2-3	
	c	02 30 35				2-3	
	d	02 32 35				2-3	
	e	02 35 00				3	
	f	02 37 40				3	

TABLE II.3 - continued.

Plate No.		Exposure time in U.T. h. m. s.	Duration of exposure in sec.	Region A	Order of grating	Seeing	Sky transparency in 10^{-6} ⊙
Jan. 20. 1963 in spot No. KKL 12368 at μ= 0.53 - continued.							
A186	a	04 16 10	15	4912	V	2	
	b	04 18 25				2	
	c	04 20 35				2	
	d	04 22 25				2	
	e	04 24 35				2	
	f	04 27 05				2	
Jan.21. 1963 in spot No. KKL 12368 at μ=0.35.							
A 189	a	03 49 25	12	4912	V	1-2	200
	b	03 53 15				2	
	c	03 56 00				2	
	d	04 02 00				1-2	
	e	04 05 55				1-2	
	f	04 07 55				1	
A190	a	04 19 20	7	5576	IV	1-2	
	b	04 22 25				1-2	
	c	04 26 20				1-2	
	d	04 31 00				1-2	
	e	04 33 50				1-2	
A191	a	04 47 25	7	5691	IV	1-2	
	b	04 50 30				1-2	
	c	04 52 30				2	
	d	05 10 15				1-2	
	e	05 21 50				2	
Feb. 9. 1963 in spot No.KKL 12375 at μ = 0.74							
A262	b	02 54 25	12	4912	V	4	
	c	02 56 15				4	
	d	02 58 00				3-4	
	e	02 59 50				4	
	f	03 01 15				4	
A263	a	03 06 15	12	4912	V	4	
	b	03 08 15				3-4	
	c	03 11 18				4	
	d	03 13 45				3-4	
	e	03 15 05				3	
	f	03 17 10				3	

TABLE II.3 - continued.

Plate No.		Exposure time in U.T. h. m. s.	Duration of exposure in sec.	Region A	Order of grating	Seeing.	Sky transparency in $10^{-6}\odot$
Feb. 9, 1963 in spot No.KKL 12375 at μ= 0.74 - continued.							
A264	b	03 25 20	5	5576	IV	3	
	c	03 27 20				3	
	d	03 29 03				3	
	e	03 30 30				3	
	f	03 33 03				3-4	
A265	a	03 39 20	4	5691	IV	3-4	
	b	03 41 00				3-4	
	c	03 42 50				3-4	
	d	03 43 45				3-4	
	e	03 45 10				3-4	
	f	03 48 35				3-4	
Feb. 10, 1963 in spot No.KKL 12375 at μ = 0.86							
A271	b	02 41 55	10	4912	V	2	
	c	02 44 00				2	
	d	02 47 20				2	
	e	02 49 50				2	
	f	02 52 15				3	
A272	b	03 02 25	3	5576	IV	2-3	
	c	03 04 25				3	
	d	03 06 00				3	
	e	03 07 15				2-3	
	f	03 09 40				3	
A273	a	03 17 30	4	5631	IV	2-3	
	b	03 19 20				3	
	c	03 21 00				3	
	d	03 23 00				2	
	e	03 25 00				2-3	
	f	03 26 30				3	
Feb. 11, 1963 in spot No.KKL 12375 at μ = 0.94							
A279	b	02 29 50	12	4912	V	3	35-40
	c	02 32 10				3	
	d	02 34 00				3-2	
	e	02 35 45				2	
	f	02 38 05				2	
A280	b	02 48 00	2	5576	IV	2-3	
	c	02 50 20				2-3	
	d	02 52 45				2-3	
	e	02 54 15				2-3	
	f	02 56 05				2	
A281	a	03 03 00	3	5691	IV	2-3	

TABLE II.3 - continued.

Plate	No.	Exposure time in U.T. h. m. s.	Duration of exposure in sec.	Region A	Order of grating	Seeing.	Sky transparency in 10^{-6} ⊙
		Feb. 11, 1963 in spot No.KKL 12375 at μ= 0.94 - continued.					
A281	b	03 04 45	3	5691	IV	2	
	c	03 06 20				2	
	d	03 08 20				2	
	e	03 10 00				2	
	f	03 11 38				2	
		Feb. 12, 1963 in spot No. KKL 12375 at μ= 0.95					
A285	b	02 29 25	12	4912	V	2-3	
	c	02 31 15				2-3	
	d	02 33 05				3	
	e	02 34 32				2-3	
	f	02 36 00				3	
A286	a	02 43 15	3	5576	IV	2	
	b	02 44 45				2	
	c	02 46 10				2	
	d	02 47 40				1-2	
	e	02 49 00				1-2	
	f	02 51 15				2	
A287	b	02 55 25	3	5691	IV	3	
	c	02 56 45				3	
	d	02 58 20				3	
	e	02 59 35				2-3	
	f	03 01 00				3	
		Feb.14, 1963 in spot No.KKL. 12375 at μ= 0.86					
A293	b	02 30 30	12	4912	V	4-5	42-50
	c	02 32 28				4	
	d	02 34 05				4	
	e	02 35 43				4-3	
	f	02 37 20				4	
A294	a	02 48 00	3	5576	IV	4	
	b	02 49 55				4	
	c	02 51 20				4	
	d	02 52 40				4	
	e	02 54 15				4	
	f	02 56 40				4-5	
A295	b	03 02 54	3	5691	IV	3	
	c	03 05 45				3	
	d	03 07 10				3	
	e	03 08 50				3	
	f	03 10 00				3	

TABLE II.3 - continued.

Plate No.		Exposure time in U.T. h. m. s.	Duration of exposure in sec.	Region A	Order of grating	Seeing	Sky transparency in 10^{-6} ⊙
Feb. 15, 1963 in spot No.KKL 12375 at μ = 0.75							
A299	b	02 32 45	12	4912	V	3-4	35-38
	c	02 33 48				4	
	d	02 35 30				4	
	e	02 37 15				4	
	f	02 39 30				4-5	
A300	a	02 45 25	3	5576	IV	3	
	b	02 48 18				3	
	c	02 49 55				3	
	d	02 51 30				3	
	e	02 52 55				3	
	f	02 54 40				3	
A301	b	03 01 00	3	5691	IV	3	
	c	03 02 25				3	
	d	03 04 10				3	
	e	03 05 40				3	
	f	03 07 40				3	
Feb. 16, 1963 in spot No.KKL 12375 at μ = 0.56							
A305	b	02 49 26	12	4912	V	3	63
	c	02 51 56				3	
	d	02 53 34				2-3	
	e	02 55 16				2	
	f	02 57 51				2	
A306	a	03 07 54	3	5576	IV	3	
	b	03 09 32				3	
	c	03 11 07				3	
	d	03 12 47				3	
	e	03 15 02				2	
	f	03 16 32				2	
A307	a	03 25 07	3	5691	IV	2-3	
	c	03 26 46				2-3	
	d	03 28 17				2-3	
	e	03 29 47				2-3	
	f	03 31 32				2-3	

for 7 minutes. The plates were thoroughly rocked during developing to avoid the Evershed Effect. Spectra taken for the study of velocity fields were in the regions of 4912 A in the fifth order and 5576 A and 5691 A in fourth order, of the grating. The details of the emulsion-filter combinations used are given in Table II.4.

2.3. The sight-line velocity determinations.

The Fraunhofer lines become very broad and diffuse under high dispersion, such as the one used in this study. For line displacement studies it is very advantageous to use high dispersion, provided we can devise some precise method of measuring these displacements in wide diffuse spectral lines. It becomes very difficult, if not impossible, to use the conventional method of measuring line positions, by bisecting the line with a micrometer cross-wise.

We tried measuring the Evershed Effect plates with the Abbe Comparator. The dispersion on these plates is about 6 to 8 mm/A, in the region of the spectrum studied. A 50 micron error in setting on the centre of a line can easily occur, especially when the contour of the line is not well defined. A 50-micron inaccuracy on the plate will introduce about 0.3 to 0.4 km/sec error in the velocities. The inaccuracies in setting on the line centre become more in the penumbral regions. The second method that we tried for measuring small Evershed shifts, was the isophotal approach. Several microphotometer scans over the spot at intervals of 0.2 mm (approximately 1" of arc) parallel to the dispersion were obtained. Equal intensity points of the profile

TABLE II.4

Details of grating order, filter and emulsion used.

Region	Grating order	Filter used	Emulsion used
4912	V	Ilford 623	Agfa Isochrom
5576	IV	Corning OG1	Agfa Isopan F
5691	IV	Corning OG1	Agfa Isopan F

were joined to yield an isophotal map of the line. From this isophotal map, we determined the shift of line in the sunspot region. Although this method is accurate, it is extremely laborious and time consuming. This method was given up in favour of another quick, convenient and precise method.

The method that is used here for measuring the sight-line velocities, utilizes essentially the principle of photographic subtraction. The principle was first used for wavelength measurements by Evershed (1913). The present method is, however, an extension of the original Evershed's positive-on-negative method, and is capable of greater precision and convenience of measurement. The essential advantage is that the accuracy of the setting is independent of the width of lines. This consideration is very important and full use of it is made in the present method. A more or less similar technique for measuring small shifts was also used by Servajean (1961).

To determine the position of a spectral line on a spectrogram, with a micrometer one sets the cross-wire at the centre of the line. In the positive-on-negative method use is made of a direct positive copy of the line, instead of a cross-wire. When the positive and negative of a line are superposed perfectly, a 'flat' or 'grey' pattern is obtained. At this position the positive profile precisely matches the negative. In any position other than 'grey' the two profiles will be displaced. We enlarged the spectrum to about 21 times, to yield a dispersion of about 130 to 170 mm/A. At this high dispersion each millimeter corresponds to about 0.56 km/sec. in velocity.

A distortion free enlargement is essential to obtain reliable results by this method. This condition was fulfilled by the availability of a Zeiss spectrum projector. This projector gives a very high quality image and has a flat field. The maximum magnification that can be obtained is about 22 times. The spectrum projector is provided with a plate carriage capable of moving in two perpendicular directions: one along the length of the plate, the X-direction, and other perpendicular to it, the Y -direction. A precision dial gauge is attached in the Y -direction to know the position precisely of the measured point on the plate. Each division of the dial gauge corresponds to some 38 kms on the disk. However, our velocity measures were made at interval of approximately 1100 kms and on some plates at intervals of 1900 kms. In the focal plane of this spectrum projector is placed a precision Hilger micrometer measuring engine. The plate to be measured is focussed on to a movable stage attached to the nut of the measuring engine. On this movable stage is mounted a direct enlarged positive of the line to be measured. The enlarged positive copies were made in the following manner. With the same slit width as that used for the spot spectra, we obtained a spectrum of the out of focus image of the sun's centre, in the three spectral regions used. Several direct enlarged positive prints of varying densities of the 3 lines, (4912 A, 5576 A & 5691 A), using the same spectrum projector and the same magnification were obtained. It is important for obtaining a correct match that the densities of the positive and negative should be proper. From the several enlarged positives of different densities, it was easy to choose a suitable print of the line.

A 6.2 mm wide direct positive print was mounted on the measuring stage, on which the enlarged negative of the line was focussed. The width of the positive, limits the height on the plate over which the velocity measurements are made. Using the shadow of the wires, it was very easy to align the measuring screw parallel to the dispersion. However, any non-parallelism was accounted for in the process of reduction, and will be described later. Due to the difference in magnifications and dispersions in the three spectral regions the velocity factor in these regions are slightly different. Table II.5 gives the dispersion and velocity factors in these regions.

This modified method of positive-on-negative, seems to be free from personal bias. Matching becomes difficult when the line acquires an asymmetric profile, especially near the penumbral boundary. However, with a little practice one can use the symmetrical side of the line profile for the purpose of obtaining the grey match.

To determine the Evershed shifts in the spot region with respect to the velocity in a remote photospheric region, the following procedure was adopted; we obtained the position of the line on the two sides of the wires, using the 'grey' match technique. The scale readings on the two sides of the spot, were fitted into a least square solution, to obtain the equation of the line of the form $x = a + by$. Any deviation from this line, measured in the X-direction, in the spot region gives directly the Doppler displacement in sunspots. Non-parallelism between the measuring screw and the dispersion can be accounted by

TABLE II.5

Details of dispersion and velocity factor
used in positive-on-negative method.

Wave-length region	Grating order	Dispersion on plate A/mm	Dispersion after magnification A/mm	Velocity factor after magnification, km/sec./mm
4912	V	0.1237	0.0060	0.360
5576	IV	0.1690	0.0080	0.426
5691	IV	0.1670	0.0078	0.415

multiplying the deviation ($X_O - X_C$) by the sine of the inclination of the line to the X-axis. In practice parallellism was found to be very good. In this method we have assured that the slit curvature over a height of 14 mm of slit is negligibly small and also that the solar differential rotation on the two sides of the spot is zero. Using Walker's (1909) or Minkowski's (1942) formula for the curvature of lines in grating spectrograph, we find a deviation in wavelength over this slit height to be less than 0.7 mA. A simple calculation shows that at B = 10°, the solar differential rotation for an interval of about 2° in latitude is less than about 10 metres per sec. Both these corrections to the velocity measures, have therefore been neglected, considering their small magnitude.

We measured the sight-line velocities in the spot region using this method. The sight-line velocity vectors are plotted in Figures II.2 through II.5, for each of the three lines. The beginning of the arrow indicates the location on the spot where the velocity was measured and the length represents the magnitude of velocity. The approximate direction of the disk centre is also indicated on each diagram. The boundaries of the umbra and penumbra are also given in these figures.

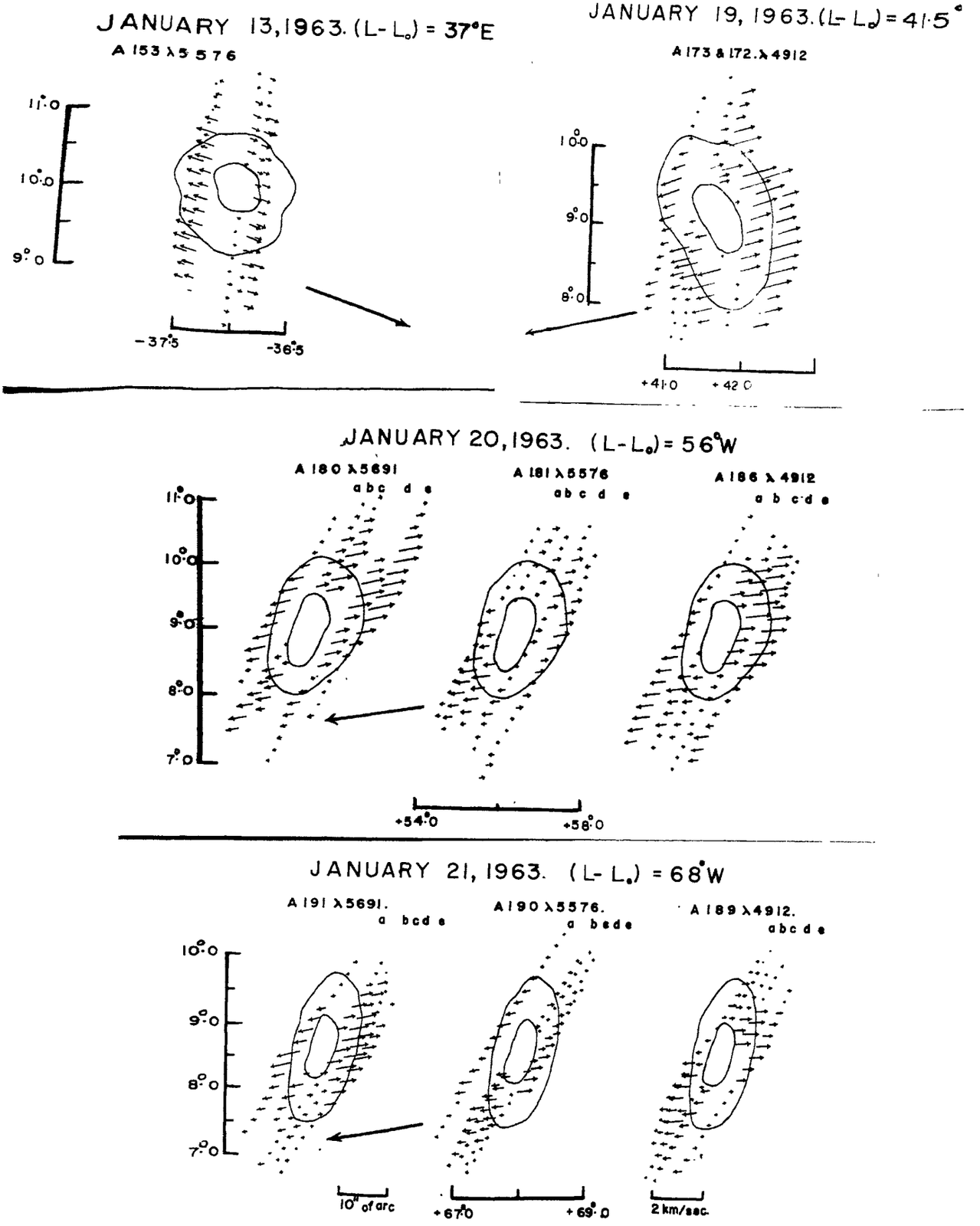

Figure II.2.- Sight-line velocity vectors
Bold arrow shows the approximate direction of the disk centre.

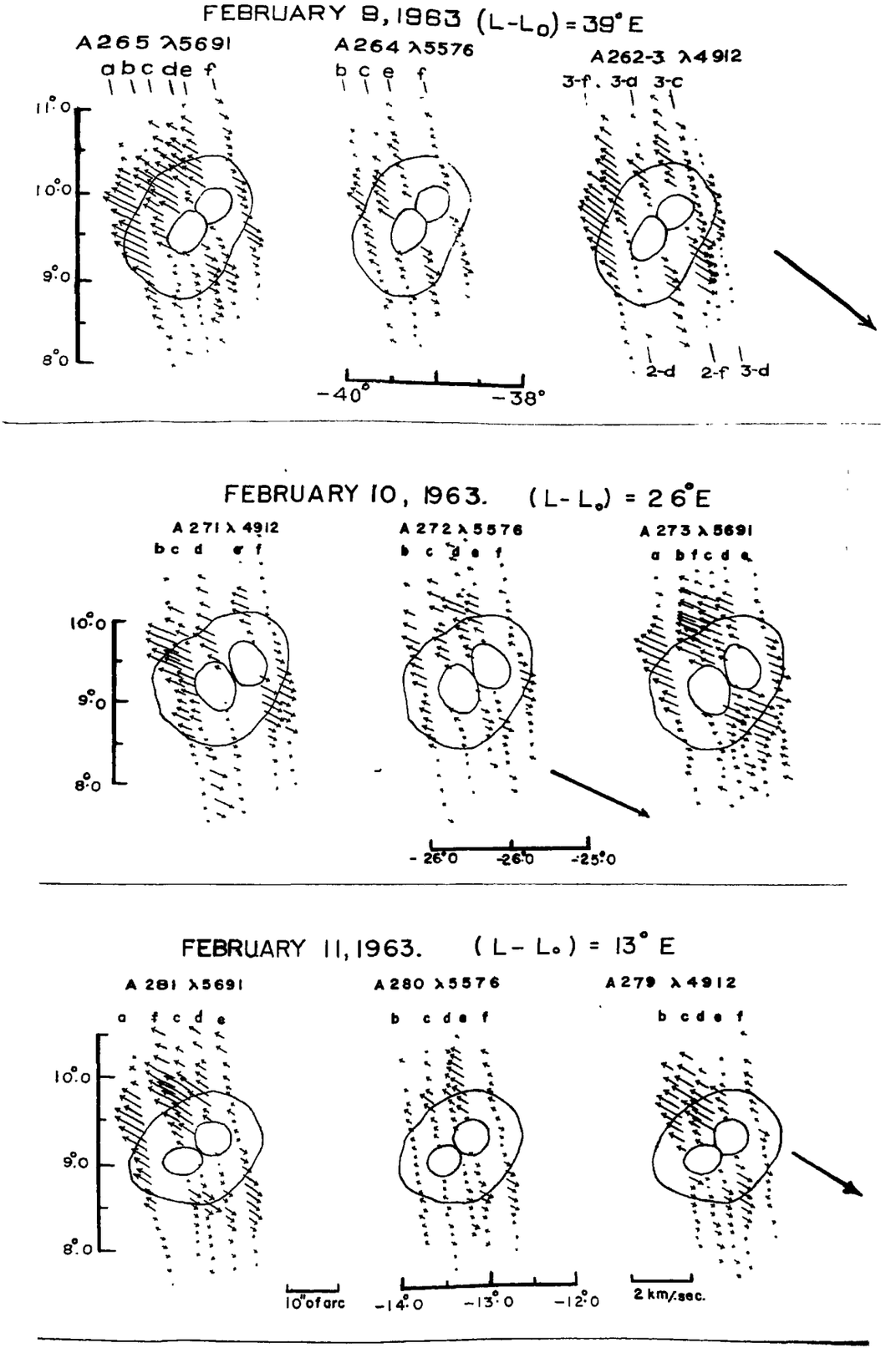

Figure II.3.- Sight-line velocity vectors
Bold arrow shows the approximate direction of the disk centre

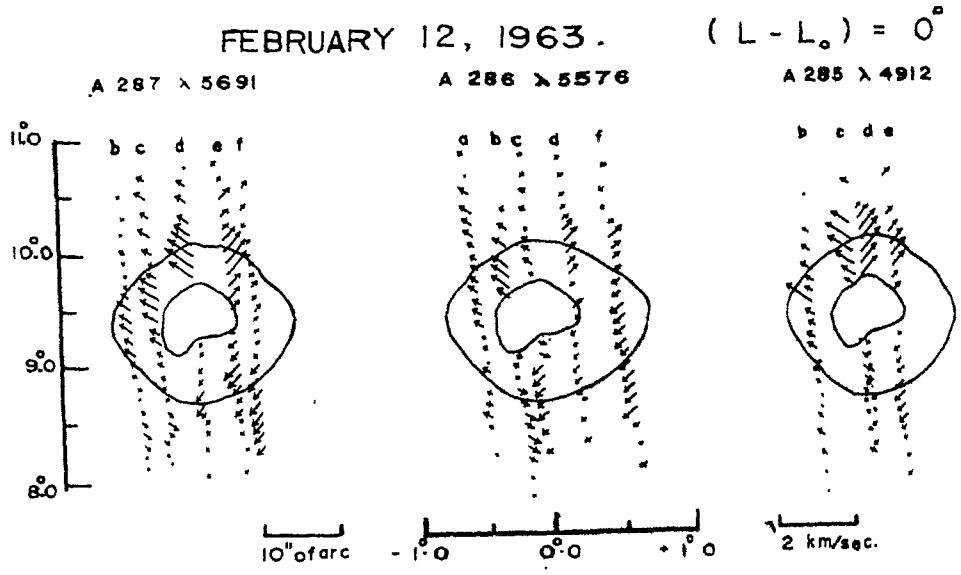

Figure 4.— Light-line velocity vectors.
Bold arrow shows the approximate direction of the [illegible]

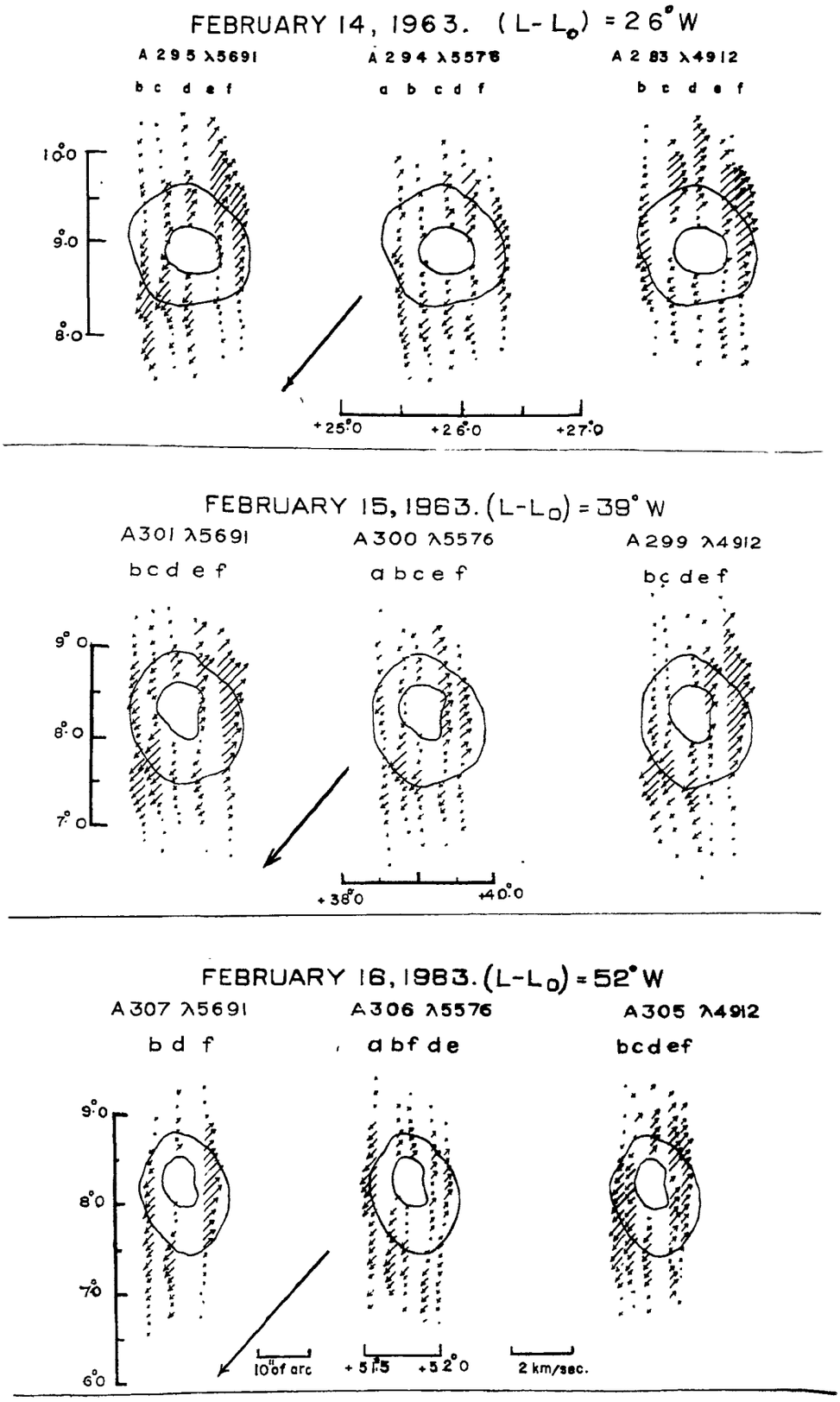

Figure II.5.- Sight-line velocity vectors.
Bold arrow shows the approximate direction of the disk centre.

CHAPTER III

Determination of component velocities in sunspots, gradient of U_{max} and spatial magnetic field.

3.1. The component velocities.

In chapter II, we have indicated the observational technique utilized for determining the spatial distribution of the sight-line velocity field in and around sunspots. The velocities that we measure on a spot spectrum, using the Doppler principle, are velocities of the line forming layers, along the line of sight. For an understanding of the physical process of motion in sunspots, we must have a knowledge of the mode of material flow in sunspots, independent of the line of sight.

In the earlier chapter, we described the procedure adopted for determining the heliographic latitude and longitude of any point in a sunspot. From the sunspot diagrams shown in Figures II.2 through II.5, giving the sight-line velocity vectors and the heliographic coordinates, we read coordinates for any desired point. To reduce the measured sight-line velocities, to velocities in the spot, we utilized the following method.

In a polar coordinate system (r, ϕ) with the centre of the umbra (B, D) as origin, the distance from the centre r, and the position angle ϕ' (measured from west through north) of any point are given by,

$$r = R_0 \left[(\Delta\lambda \cos B)^2 + (\Delta B)^2 \right]^{\frac{1}{2}} \qquad (3\text{-}1)$$

$$\text{and } \tan\phi' = \frac{\Delta B}{\Delta\lambda \cos B} \qquad (3\text{-}2)$$

where R_0 is km/degree on the solar surface, and ΔB and $\Delta\lambda$ are

the differential heliographic coordinates of a point, measured from the centre of the umbra. Kinman (1952) has shwon that the flow of material in spots has a cylindrical symmetry about the edge of the umbra. In the case of symmetrical round spots it is justifiable to assume that the motion will have a cylindrical dsymmetry about the centre of the umbra also. Working on this hypothesis, we have grouped the measured points around the sunspots into annular zones of width 1000 kms on plates taken on January 20 and 21, 1963 and into zones 750 kms wide on plates exposed during February. The number of annular zones used depended on the total number of points measured in the sunspot region. By choosing annular zones of width 1000 kms or 750 kms, we could arrange to have at least 5 to 6 points in each zone. The number of measured points in each zone is important, since, use of a large number of points reduces the r.m.s. error of determinations. In most of the spots, we measured velocities upto about 15,000 to 18,000 kms from the umbral centre.

All the three component velocities in a rectangular coordinate system can be determined using the method of Plaskett (1952). This method has been used by Kinman (1952, 1953), by Servajean (1961) and by Holmes (1961), for the study of Evershed Effect. From one observed velocity parameter - the sight-line velocity - all the three velocity components referred to a fixed coordinate system can be derived, by this method. In the present thesis also, we have made use of this method to obtain the three component velocities.

Let us assume a rectangular coordinate system, with the

origin of the system at the centre of the sunspot. In Figure XII.1, let O be the centre of the spot. Let the X-axis be parallel to the direction of the solar rotation, and the Y-axis perpendicular to it and in the plane of the sunspot surface. The Z-axis is directed outwards normal to the solar surface. We are interested in determining the component velocities u, v and w, where 'u' is the velocity directed radially away from the spot centre, v the tangential velocity at the point of interest, and w the velocity directed perpendicular to the solar surface. It is convenient to use the cylindrical coordinate system, to consider the motion in spots. The three cylindrical velocity components u, v and w are denoted by $u = \dot{r}$, $v = r\dot{\phi}$ and $w = \dot{z}$, where r, ϕ and z are the cylindrical coordinates. The corrected sight-line velocity is given by

$$\begin{aligned} V &= u(\cos\phi' \cos\gamma_1 + \sin\phi' \cos\gamma_2) \\ &+ v(\cos\phi' \cos\gamma_2 - \sin\phi' \cos\gamma_1) \\ &+ w \cos\gamma_3 \end{aligned} \qquad (3\text{-}3)$$

where $\cos\gamma_1$, $\cos\gamma_2$, and $\cos\gamma_3$ are the direction Cosines of the line of sight directed from the observer to the measured point on the solar surface. The direction cosines are given by the following expressions, if we neglect the small angle θ_1 or the angle subtended at the observer, by the spot and the sub-terrestrial point.

$$\begin{aligned} \cos\gamma_1 &= \sin(L-L_0)\cos B \\ \cos\gamma_2 &= \sin B \cos B_0 \cos(L-L_0) - \cos B \sin B_0 \\ \cos\gamma_3 &= -\cos\theta \end{aligned} \qquad (3\text{-}4)$$

For the spots observed the value of θ_1 does not exceed $0.^{\circ}1$. (L-Lo) and the heliographic latitude B, for any measured point on the sunspot were obtained from the sunspot maps. B_0 and L_0 are tabulated for each day in the Nautical Almanac.

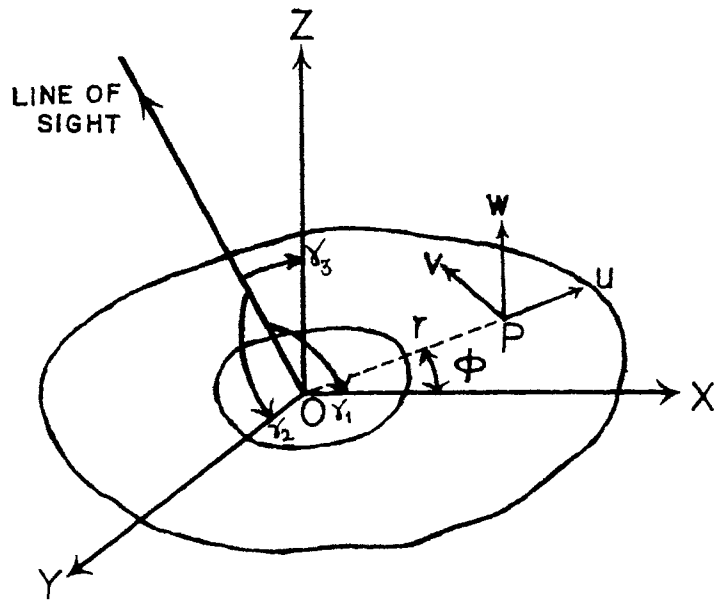

Figure III.1.

The observed velocities need to be corrected for the observer's motion and for solar rotation. The corrected sight-line velocity is given by

$$V = V^* - U_s \cos \gamma_1 + C_1 + \Delta \qquad (3\text{-}5)$$

where V^* is the observed sight-line velocity, U_s the velocity due to solar rotation, at the measured point on the disk, and is given by (Hart 1959),

$$U_s = 2 \cos B \, (1 - 0.229 \sin^2 B) \qquad (3\text{-}6)$$

C_1 is the correction due to the observer's motion and compensates both the earth's motion about its axis as well as the rotation of the earth-moon system about the centre of mass of the solar system. Δ is the correction due to the limb effect. Neglecting the limb effect correction Δ, since it is a very small quantity for disk positions of the spot observed, the corrected sight-line velocity is given by,

$$V = V^* - U_s \cos\gamma_1 - 0.4571 \cos\delta_0 \sin H - 1732.34 \left[\dot{X} \cos\delta_0' \cos\alpha_0' + \dot{Y} \cos\delta_0' \sin\alpha_0' + \dot{Z} \sin\delta_0' \right] \qquad (3\text{-}7)$$

The third term gives the contribution of the earth's rotation about its axis in km/sec. for Kodaikanal. The fourth term represents the velocity correction due to the rotation of earth-moon system about the centre of mass of the solar system (Schlesinger 1899).

Equation (3-3) involves three unknown quantities u, v and w. To determine these we should have at least three equations of the type (3-3). We have assumed at the onset that the motion of material has a cylindrical symmetry about the spot centre. This

implies that all the points equidistant from the centre of the spot, satisfy the equation of condition (3-3). For each of the measured points in an annular zone, we have the following equations of condition,

$$\left.\begin{aligned} V_1 &= ux_1 + vy_1 + wz_1 \\ V_2 &= ux_2 + vy_2 + wz_2 \\ \cdots &\quad \cdots \quad \cdots \quad \cdots \\ V_n &= ux_n + vy_n + wz_n \end{aligned}\right\} \qquad (3\text{-}8)$$

where $x = (\cos\phi' \cos\gamma_1 + \sin\phi' \cos\gamma_2)$

$y = (\cos\phi' \cos\gamma_2 - \sin\phi' \cos\gamma_1)$

$z = (\cos\gamma_3) = -\cos\theta$.

Equations (3-8) can be solved by the method of least squares to yield u, v & w.

In constructing a rectangular coordinate system, with O as origin, Figure III.1, we assumed the sunspot surface to be a p plane. This assumption is valid, as the spots observed are not greater than 3 degrees in diameter. We notice in equation (3-2) that the coefficient of w, cos γ_3 (= $-\cos\theta$) is independent of ϕ' and constant over the plane spot surface. Following Servajean (1961), we have made cos γ_3 constant and equal to unity. We then obtain the following solution by the method of least squares for u, v and w.

$$u = \frac{a_1 \Sigma Vx + b_1 \Sigma Vy + c_1 \Sigma V}{d}$$

$$v = \frac{a_2 \Sigma Vy + b_2 \Sigma V + c_2 \Sigma Vx}{d}$$

$$w = \frac{a_3 \Sigma V + b_3 \Sigma Vx + c_3 \Sigma Vy}{d}$$

where $d_1 = (\Sigma y)^2 - n \Sigma y^2$

$$a_2 = (\Sigma x)^2 - n \Sigma x^2$$
$$a_3 = (\Sigma xy)^2 - \Sigma x^2 \Sigma y^2$$
$$b_1 = c_2 = n \Sigma xy - \Sigma x \Sigma y$$
$$b_2 = c_3 = \Sigma x^2 \Sigma y - \Sigma xy \Sigma x$$
$$b_3 = c_1 = \Sigma y^2 \Sigma x - \Sigma xy \Sigma y$$

and

$$d = \Sigma x^2 (\Sigma y)^2 + \Sigma y^2 (\Sigma x)^2 + n(\Sigma xy)^2 - n\Sigma x^2 \Sigma y^2 - 2 \Sigma xy \Sigma x \Sigma y$$

A programme in FORTRAN language for the IBM 1620* was written to calculate the direction cosines, position angle ϕ and other quantities, used for solving equations (3-8). In this programme instructions were coded to punch out data required for calculating the root mean square errors. The punched out cards were re-run to obtain the root mean square error for each of the three component velocities. Use of the IBM 1620 reduced considerably the labour required for computing the component velocities and their r.m.s. errors, in about 270 annular zones.

The results of the component velocities are given and discussed in section (3-4) of this chapter.

3.2. Determination of mean depths of formation of lines.

An absorption line in the solar spectrum is formed over a considerable thickness of the solar atmosphere. Individual strata contribute to the formation of a line, depending on the physical parameters of each layer. For determining the depth of formation of a line, we must have a knowledge of the model of the atmosphere, i.e. the dependence of temperature, pressure and the coefficient of continuous absorption on the depth. Together with this

---

*IBM 1620 facilities of the Physical Research Laboratory, Ahmedabad were utilized.

information, the parameters of the atomic transition giving rise to the spectral line under study, enable the evaluation of the depth of contributing layers. Minnaert (1948) and Pecker (1951) have developed theories for calculating the mean depths of formation of faint lines in the solar atmosphere. The mean optical depth, $\bar{\tau}$ mean is defined as

$$\int_0^{\bar{\tau}_{mean}} I \, d\bar{\tau} = \int_{\bar{\tau}_{mean}}^{\infty} I \, d\bar{\tau}$$

From the mean optical depth $\bar{\tau}$ mean one can easily derive the mean geometrical depth $\bar{h}$, of the line forming layer. The mean optical depth, can be determined from a knowledge of the contribution curves for the line in question. The bisector of the area under the contribution curve, gives directly the logarithm of the mean optical depth. We have utilized this procedure for determining $\bar{\tau}$ of the spot lines used for velocity measurement.

As mentioned earlier, a model of the atmosphere, giving the variation of electron pressure and temperature with optical depth, is a necessary prerequisite for the calculation of the mean depths of formation of the individual lines. Makita (1963) has recently worked out a model for sunspot penumbra, with the aid of photoelectric and photographic spot spectra. We have used the Makita model for computing the contribution function and thereafter the mean geometric depth $\bar{h}$, of formation of 4912 A and 5691 A lines. Several workers Michard (1953), Minnaert (1953), Mattig (1958) have computed models that yield physical parameters of sunspots. However, these models refer entirely to

the physical conditions in sunspot umbrae only. Makita's model on the other hand relates to the physical conditions in the penumbra and hence is well suited for our purpose. We give in Table 3.1 details of Makita's penumbra model.

The intensity at a point on the line profile is

$$I_{\Delta\lambda(0,\mu)} = \int_0^\infty B_{\lambda_0}(h') \left[exp - \int_0^{h'} (k_{\lambda_0} + k_{\Delta\lambda}) P.\rho. \frac{dh'}{\mu} \right] (k_{\lambda_0} + k_{\Delta\lambda}) P.\rho. \frac{dh'}{\mu} \qquad (1)$$

or

$$I_{\Delta\lambda(0,\mu)} = \int_0^\infty B_{\lambda_0}(\tau') \left[exp - \int_0^{\tau'} \left(1 + \frac{k_{\Delta\lambda}}{k_{\lambda_0}}\right) \frac{d\tau'}{\mu} \right] \left(1 + \frac{k_{\Delta\lambda}}{k_{\lambda_0}}\right) \frac{d\tau'}{\mu} \qquad (2)$$

where

B_{λ_0} = the Plank function

ρ = the number of hydrogen atoms per gram of solar material

μ = $\cos\theta$, θ is the angle between the solar radius at the point of observation on the disk, and the line of sight.

k_{λ_0} = continuous absorption coefficient per atom of hydrogen

$k_{\Delta\lambda}$ = selective absorption coefficient per atom of hydrogen

ρ = density of solar material

h' = geometrical depth.

we then obtain

$$I_{\lambda_0(0,\mu)} - I_{\Delta\lambda(0,\mu)} = \int_0^\infty B(\tau') \left\{ \left[exp - \left(\frac{\tau'}{\mu}\right) \right] - \left[exp - \int_0^{\tau'} \left(1 + \frac{k_{\Delta\lambda}}{k_{\lambda_0}}\right) \frac{d\tau}{\mu} \right] \right\} \frac{d\tau'}{\mu}$$
$$- \int_0^\infty B(\tau') \left[exp - \int_0^{\tau'} \left(1 + \frac{k_{\Delta\lambda}}{k_{\lambda_0}}\right) \frac{d\tau}{\mu} \right] \left(\frac{k_{\Delta\lambda}}{k_{\lambda_0}}\right) \frac{d\tau'}{\mu} \qquad (3)$$

Equation (3) represents the difference between the continuum intensity $I_{\lambda_0(0,\mu)}$ and the intensity of a point on the line profile.

The residual intensity

$$r = \frac{I_{\lambda_0(0,\mu)} - I_{\Delta\lambda(0,\mu)}}{I_{\lambda_0(0,\mu)}} \qquad (4)$$

TABLE III.1

Makita's sunspot penumbra model, used in this study.

$\log \tau$	τ	T	$\log p_e$	$\log p_g$	$\log \rho$	h(km)
-3.0	.0010	3810	-0.69	3.51	-7.61	0.0
-2.8	.0016	3880	-0.61	3.61	-7.60	1.03×10
-2.6	.0025	3960	-0.48	3.71	-7.52	2.41
-2.4	.0040	4050	-0.34	3.81	-7.43	3.99
-2.2	.0063	4150	-0.19	3.91	-7.34	5.41
-2.0	.0100	4240	-0.085	4.01	-7.31	7.25
-1.8	.0159	4325	0.04	4.09	-7.29	9.49
-1.6	.0251	4400	0.145	4.20	-7.18	1.21×10^2
-1.4	.0398	4480	0.235	4.275	-7.12	1.49
-1.2	.0631	4540	0.32	4.35	-7.10	1.83
-1.0	.1000	4620	0.415	4.42	-7.00	2.23
-0.8	.1585	4890	0.545	4.43	-7.00	2.78
-0.6	.2512	5180	0.74	4.53	-6.90	3.48
-0.4	.3981	5470	0.96	4.66	-6.75	4.20
-0.2	.6310	5740	1.19	4.80	-6.59	4.81
0.0	1.0000	6020	1.415	4.84	-6.53	5.39
0.2	1.5050	6360	1.70	4.93	-6.41	6.01
0.4	2.5120	6760	2.07	5.07	-6.25	6.51
0.6	3.9810	7310	2.50	5.20	-6.08	6.81

can be written in the form indicated by Pecker (1951),

$$r = \int_0^\infty G.\psi.\left(\frac{k_{\Delta\lambda}}{k_{\lambda_0}}\right)\frac{d\tau'}{\mu} \tag{5}$$

where G is the weighting function given by

$$G = \frac{\int_{\tau'}^\infty B(\tau)\left[\exp-\left(\frac{\tau}{\mu}\right)\right]\frac{d\tau}{\mu} - B(\tau)\left[\exp-\left(\frac{\tau'}{\mu}\right)\right]}{\int_0^\infty B(\tau)\left[\exp-\left(\frac{\tau'}{\mu}\right)\right]\frac{d\tau'}{\mu}} \tag{6}$$

and ψ is the saturation function

$$\psi = \exp-\int_0^{\bar{\tau}}\left(\frac{k_{\Delta\lambda}}{k_{\lambda_0}}\right)\frac{d\tau}{\mu} \tag{7}$$

The source function may be written as

$$B(\tau) = a + b\tau + cE_2(\tau) \tag{8}$$

where $E_2(r)$ is the exponential integral. Integrating by parts the numerator of equation (6) and substituting (8) in (6), we have

$$G = \frac{B(\tau)\exp-\left(\tau'/\mu\right)+\int_{\tau'}^\infty \frac{dB(\tau)}{d\tau}\exp\left(-\frac{\tau}{\mu}\right)d\tau' - B(\tau)\exp\left(-\frac{\tau'}{\mu}\right)}{\int_0^\infty a\exp-\left(\tau'/\mu\right)\frac{d\tau}{\mu} + \int_0^\infty b\tau.\exp\left(-\frac{\tau}{\mu}\right)\frac{d\tau}{\mu} + \int_0^\infty cE_2(\tau)\exp\left(-\frac{\tau}{\mu}\right)\frac{d\tau}{\mu}} \tag{9}$$

$$= \frac{\int_{\tau'}^\infty \frac{dB(\tau)}{d\tau}\exp\left(-\frac{\tau}{\mu}\right)d\tau'}{a + b\mu + c\left[1 - \mu\ln\left(1+\frac{1}{\mu}\right)\right]} \tag{10}$$

substituting $\frac{dB(\tau)}{d\tau}$ from equation (8) in (10)

$$G = \frac{\int_{\tau'}^\infty b\exp\left(-\frac{\tau}{\mu}\right)d\tau' + \int_{\tau'}^\infty cE_2'(\tau)\,e^{-\tau/\mu}d\tau}{a + b\mu + c\left[1 - \mu\ln\left(1+\frac{1}{\mu}\right)\right]} \tag{11}$$

$$G = \frac{b\mu \exp(-\tau/\mu) - c\int_{\tau}^{\infty} E_1(\tau)\exp(-\tau/\mu)\cdot d\tau}{a + b\mu + c\left[1 \mp \mu \ln(1+1/\mu)\right]}$$

$$= \frac{b\mu \exp(-\tau/\mu) - c\int_{\tau}^{\infty} \exp(-\tau/\mu)d\tau \cdot \int_{1}^{\infty} \exp(-x\tau)\frac{dx}{x}}{a + b\mu + c\left[1 \mp \mu \ln(1+1/\mu)\right]}$$

From the property of exponential integrals and chaing the order of integration and integrating we obtain

$$G = \frac{b\mu \exp(-\tau/\mu) - c\int_{\tau}^{\infty} \frac{\exp -\tau\left(\frac{1}{\mu}+x\right)}{x\left(1/\mu + x\right)}\cdot dx.}{a + b\mu + c\left[1 \mp \mu \ln(1+1/\mu)\right]}$$

$$G = \frac{\mu \exp(-\tau/\mu)\left[b - cE_1(\tau)\right] + c\mu E_1\left(\tau + \frac{\tau}{\mu}\right)}{a + b\mu + c\left[1 \mp \mu \ln(1+1/\mu)\right]} \qquad (12)$$

To determine G, we have made use of the solar limb darkening observations of Pierce and Waddell (1961). From a knowledge of the limb darkening constants a, b, and c, we compute G for the wavelength 5000 A at five disk positions. These weighting functions were utilized in the computation of mean depths of formation of lines 4912 A, 5691 A. The values of the constant a, b and c given by Pierce and Waddell are as follows:

a = + 0.68897
b = + 0.47873
c = -0.54651

Ideally, we should have taken limb darkening observations over the

sunspot penumbra. However, the photoelectric results of Makita and Morimoto (1960) indicate that the penumbral limb darkening curve is parallel to the solar limb darkening curve. We believe that no sensible error would have occurred on this score.

Ten Bruggencate et. al (1955) have shown that for numerical integration of equation (5), it is more convenient to integrate over a $\log \tau$ scale, instead of over τ

Let $x = \log_e \tau$, $dx = \frac{d\tau}{\tau}$

$$d\tau = \tau\, d(\log_e \tau)$$

$$\text{or } d\tau = \frac{\tau}{\text{Mod}}\, d(\log_{10} \tau) \qquad (13)$$

Equation (5) can be written in this form

$$r = \int_{-\infty}^{\infty} \frac{G}{\mu} \cdot \left(\frac{k_{\Delta\lambda}}{k_{\lambda 0}}\right) \tau \cdot \frac{\psi}{\text{Mod}} \cdot d(\log_{10} \tau) \qquad (14)$$

and

$$\psi = \exp - \int_{-\infty}^{+\log \tau'} \left(\frac{k_{\Delta\lambda}}{k_{\lambda 0}}\right) \frac{\tau}{\mu} \cdot \frac{1}{\text{Mod}} \cdot d(\log_{10} \tau) \qquad (15)$$

The selective absorption coefficient $k_{\Delta\lambda}$ per hydrogen atom is given by

$$k_{\Delta\lambda} = \frac{\sqrt{\pi} e^2 \lambda_0^2}{mc^2} \cdot A \cdot f \cdot \frac{N_{ia}}{N_a} \cdot \frac{1}{\Delta\lambda_D} \cdot \exp - \left(\frac{\Delta\lambda}{\Delta\lambda_D}\right)^2 \qquad (16)$$

We assume that our measures of the line displacements refer to only the core of the line, where $\Delta\lambda = 0$. Expression (16) is now given by

$$k_{\Delta\lambda} = k' \cdot A \cdot f \cdot \frac{N_{ia}}{N_a} \cdot \frac{1}{\Delta\lambda_D} \qquad (17)$$

where $$k' = \frac{\sqrt{\pi} \cdot e^2 \lambda_0^2}{m c^2}$$

A is the number of atmos of the element per hydrogen atom, f is the oscillator strength, N_{ia} is the number of atmos of the element in the energy level corresponding to the transition responsible for the line, N_a is the total number of atoms of that element, and $\Delta\lambda_D$ is the Doppler width given by

$$\Delta\lambda_D = \frac{\lambda}{c}\sqrt{\frac{2RT}{\mu}}$$

where the μ is the atomic weight of the element, c/λ the frequency of the line, and T the effective temperature, assumed to be $\theta = 1.02$ in our case and R the gas constant. We have neglected microturbulence effects because of their unknown contribution.

If we write

$$K = \frac{k' \cdot A \cdot f}{Mod} \qquad (18)$$

equation (14) can be written as

$$r = K \cdot \int_{-\infty}^{\infty} G \cdot \frac{\tau}{\mu} \cdot \frac{1}{k_{\lambda_0}} \cdot \frac{N_{ia}}{N_a} \cdot \psi \cdot \frac{1}{\Delta\lambda_D} \cdot d(\log_{10}\tau) \qquad (19)$$

The quantity $\left(\frac{N_{ia}}{N_a}\right)$ in equation (19) is directly obtained from the combined Saha and Boltzmann equations. We calculated $\left(\frac{N_{ia}}{N_a}\right)$ for each

of the temperature and electron pressure values in the sunspot penumbra model (Makita 1963) and for each of the three lines, by the equation

$$\left(\frac{N_{ia}}{N_a}\right) = \frac{P_e\, g_{ia} \exp - \chi/kT}{\left[B_0(T)\, P_e + Q\, T^{5/2}\, 2\, B_1(T) \exp - I/kT\right]} \quad (20)$$

where P_e is the electron pressure,

g_{ia} the statistical weight of the energy level

$B_0(T)$ and $B_1(T)$ the partition function of the neutral and ionized atoms respectively

and $Q = \frac{(2\pi m)^{3/2}\, k^{5/2}}{h^3}$

The partition functions for FeI and NiI were obtained from Claas (1950). The Rowland tables identify 5691 line to be a blend of FeI and NiI. In this study we assume 5691 A to be the result of the $(y^5F - g^5D)$ transition of FeI.

We neglected the contribution to the continuous absorption, due to the neutral hydrogen atom. The contribution by neutral hydrdgen atom in this wavelength region is small. Besides, the penumbral model used ignores the effects of neutral H absorption. The contribution due to the negative hydrogen ion was taken from Chandrasekhar and Breen's tables (1946). The H^- absorption for our electron pressure P_e values were graphically interpolated. At it was not possible to obtain laboratory determined f values for our lines, we obtained these values from Wright's (1944) sola curve of growth. The equivalent width of these lines were taken from the Utrecht photometric catalogue (196). The saturation

functions, ψ, were obtained by numerical integration of equation (15). The contribution function is given by

$$\delta\tau_{0\mu}^{\tau} = G\left[\frac{K}{\mu}\frac{\tau}{\Delta\lambda_D}\cdot\frac{1}{Pe\,\alpha(H^-)}\cdot\frac{1}{\left(\frac{N_{oH}}{N_H}\right)}\cdot\frac{N_{Ia}}{N_a}\right]\psi \qquad (21)$$

$\left(\frac{N_{oH}}{N_H}\right)$ is the ration of the number of hydrogen atoms in excited to the ground level. Figure 3.2 shows the contribution curves for the central depth, for each of the two lines, at μ= 0.35, 0.55, 0.75, 0.85 and 0.95. The bisection of the area under each contribution curve gave immediately themean optical depth of formation of the line, at a particular disk position in the penumbra of spot. The effective depth of formation of 5576.101 A line of FeI (Rowland intensity 4), in the sunspot penumbra seems to lie much higher than the other two Zeeman insensitive lines, used in this study. The Makita model at our disposal does not permit the yielding of a complete contribution curve for this line. Hence, for U_{max} gradient determinations we have considered only the two faint Zeeman insensitive lines 4912.027 A and 5691.508 A. From Table III.1 we directly obtain the mean geometrical depths for the lines. In Table III.2, we give the mean optical and geometrical depth of formation, of these lines, at five μ values.

3.3. Details of the sunspots studied.

In this section we briefly describe the details of the sunspots in which we have determined the velocity and magnetic fields. As mentioned in an earlier chapter, we obtained spectra during two successive passages of a spot group. Our observations

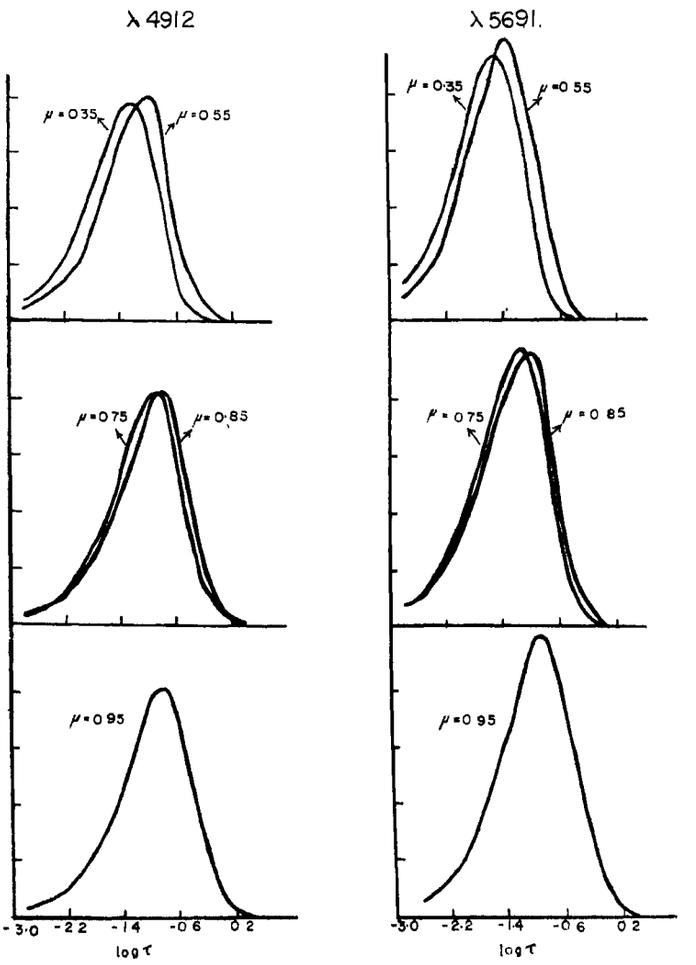

Figure 1 .2.- Contribution curves for 4912.027 Å and 5691.503 Å lines at five values in the penumbra.

TABLE III.2

Mean optical and geometrical depths of formation of lines, using Makita's penumbral model.

μ	4912.027 A		5691.508 A	
	$\log \tau$	km	$\log \tau$	km
0.95	-0.96	235	-1.18	188
0.85	-0.98	230	-1.24	175
0.75	-1.04	215	-1.29	166
0.55	-1.21	180	-1.42	145
0.35	-1.36	155	-1.62	117

of velocity and magnetic fields made during the second and third pass of the same spot group across the disk makes the problem very interesting. This investigation enables us to study changes in the velocity and magnetic field configuration, with the evolution of a spot. However, during the second and third pass, this spot had become stable.

Kodaikanal photoheliogram records show that Kodaikanal spot No.12358 first appeared around December 18,1962 at about $L-L_0 = 14^0$ east and receded beyond the western limb on December 25. This spot group was in McMath plage region 6649. In this plage region only one subflare (importance 1$^-$) was observed on December 20 as seen from the CRPL list of solar flares. The same spot group appeared on January 9, 1963 on the eastern limb and was designated in our records as Kodaikanal spot No.12368 (KKL 12368). Central meridian passage of this spot was on January 16. Until January 13 no apparent change in the shape and size could be noticed in the spot group. From January 9 to 14 only two small subflares are reported in CRPL data. From January 14 onwards rapid changes in the shape and size, as well as additional spots, started appearing around this spot group. On January 15 two large spots developed in this region and on January 16 another spot joined to make the whole spot region very complex. During this developing phase of spot group KKL 12368, more than seven subflares have been reported in the CRPL reports. From January 18 onwards the spot group started decreasing in area and also some of the newly formed spots vanished, leaving behind on January 19 only the single spot that appeared on the eastern limb and a small spot south of it. Subsequent to January 19

until it went beyond the western limb, no flare activity was reported. It appears that from January 19 onwards the spot group KKL 12368, acquired the stable and mature phase of its life. During this second passage of the spot across the disk, we determined the velocity fields on January 13, 19, 20 and 21. The observed sight-line velocity vectors are given in chapter II. Difference in velocity fields, between the pre-development and post development phases coul d be noticed. The disk positions of the spot on January 13 and 19 have almost the same distances from the disk centre and were on either side of the meridian. We have determined the component velocities in the spots observed on January 20 and 21.

The same spot group again appeared on the eastern limb on February 3 and is designated in our records as KKL 12375 and was on its third passage. This time it appeared as a single round symmetrical spot. We observed this spot on February 9, 10, 11, 12, 14, 15 and 16 and obtained both the spatial velocity and magnetic field configurations. The spatial velocity field measurements were made using the three Zeeman insensitive lines. Sight-line velocity vectors are given in chapter II. For spatial magnetic field measurements, either of the two lines 6303 A and 6173 A were used. Spatial magnetic field maps are given in section 3.7.

Due to poor weather conditions we did not observe this spot, until February 9 ($L-L_0 = 40^{\circ}E$). After the rainy spell seeing conditions and sky transparency were subperb on February 9. The umbra of this spot (KKL 12375) appeared split in two, surrounded by a common penumbra. This appearance of the spot remained till

February 11, and around February 12 ($L-L_0 = 0^0$) the two umbrae coalesced to form a single umbra. No change in shape or size other than this could be noticed during the rest of its passage across the disk. To decide as to whether the two umbrae were part of the same umbra or were two separate umbrae, we examined the magnetic field plates. As mentioned earlier, we also obtained spatial magnetic field plates on almost all days when we obtained velocity field plates. Zeeman spectra taken on 9, 10 and 11 February, with the slit crossing the juction of the two umbrae showed a larger magnetic field than on slit positions crossing the individual umbrae. The polarity of the two umbrae were the same. These observations of magnetic field and the shape of the spot convinced us that the existence of two umbrae was illusory. It was in fact a single umbra that appeared split, because of some penumbral material covering the umbra. On February 12 and later the two umbrae appeared as single. We therefore assume the centre of the whole umbra as representative of the spot's centre. KKL 12375 disappeared beyond the western limb around February 19 and reappeared on March 3 on the eastern limb, with more or less the same shape and size that it had on the previous passage. The only flare reported after January 18 in the CRPL lists, associated with this spot was on March 5. Since March 5 till the spot vanished on the disk around March 14-15, 10 subflares of importance 1 to 1^- were reported. From the flare data obtained and the configuration of spot group, it is definite that from 19 January to March 3, this spot was in the stable and mature phase of its life. This is in agreement with our earlier findings (Bhatnagar and Punetha 1963) that less intense flares of importance 1 to 1^- occur during the

development and declining phases of the spot's life.

From the above discussion it is well established that the two spots observed during January and February 1963, were the same. The variation in the velocity configuration at the same disk position, but during the two passages, may serve as an indication of the changes in velocity field pattern, with the age of spot.

Using the method described in section 3.1 of this chapter, we calculated with the aid of the IBM 1620 the component velocities, u, v and w, and also their r.m.s. errors. These velocities and the r.m.s. errors are plotted in Figures III.3 through III.9. In the following, we discuss the run of these individual component velocities in sunspots. From the knowledge of the mean depths of formation of the lines 4912 A and 5691 A, we obtain the gradient of the maximum radial velocity (U_{max}) variation with depth. This is given in the next section along with the radial velocity pattern in spots.

3.4. Radial velocity component u.

The radial velocity u, is the component of the sight-line velocity parallel to a radius vector of the sunspot, and in the plane of the solar surface. It is this component velocity that is most important in our investigation of the Evershed Effect. By the method given in section 3.1, we uniquely determine the magnitude of this component u. As, has been stated earlier the measured points in and around the spot were grouped in annular zones, at arbitrary distances from the spot centre. For each of the annular zones, we then obtain all the three component velocities u,v and w.

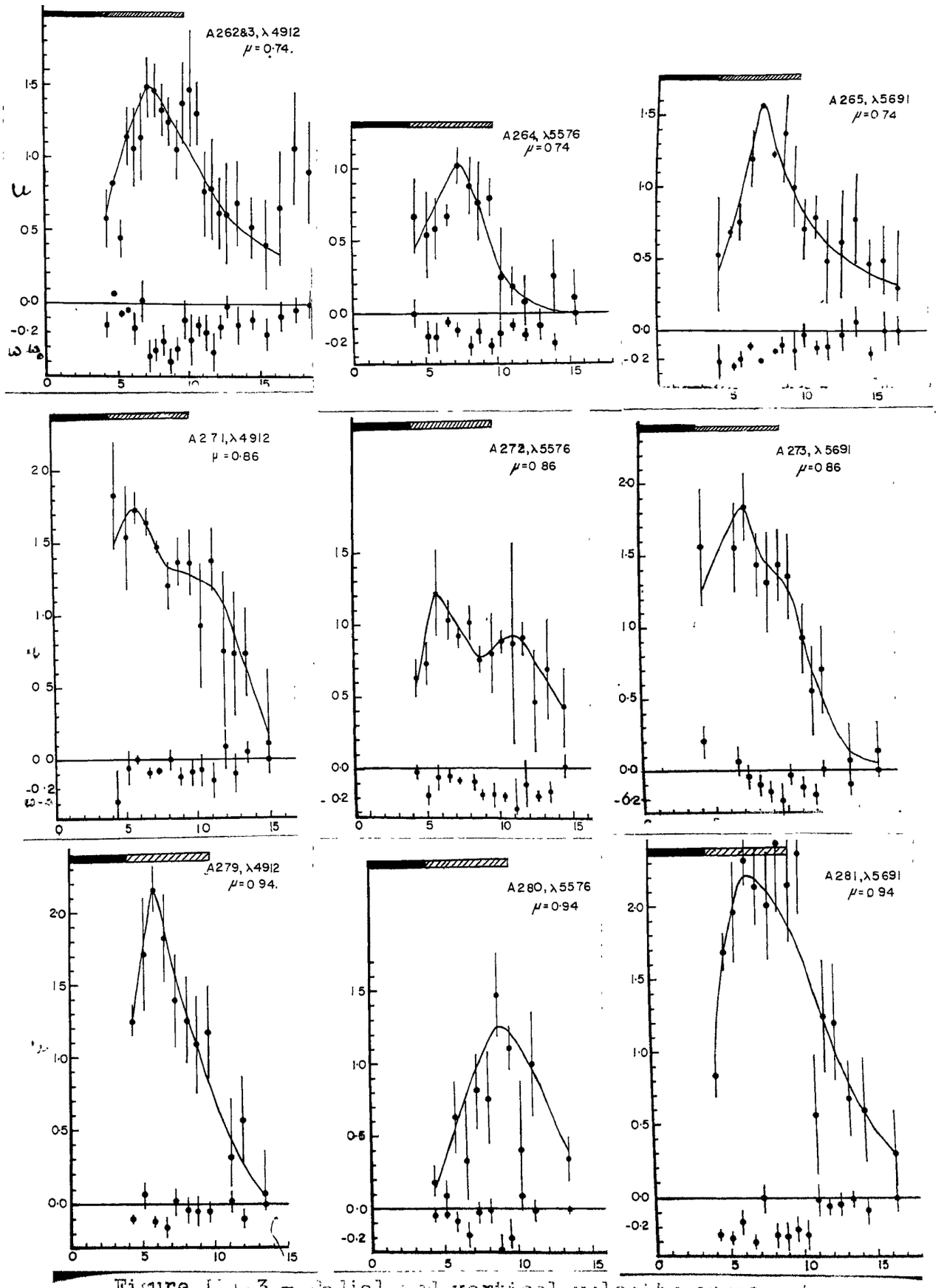

Figure III.3.- Radial and vertical velocity components, as a function of distance from the centre of the spot; abscissae in units of one thousand kilometres and ordinate in km/sec.

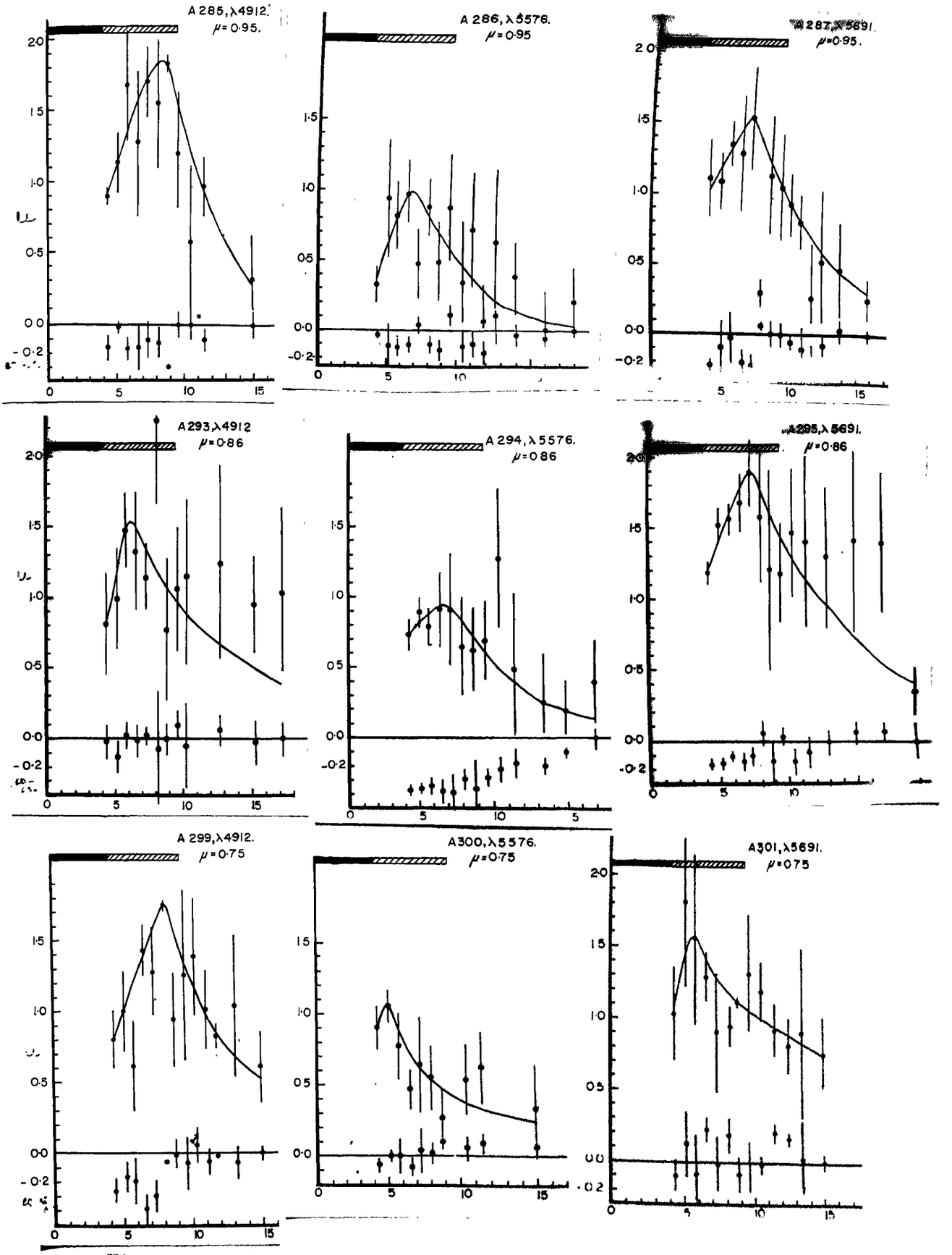

Figure 11.4.- Radial and vertical velocity components, as a function of distance from the centre of the spot; abscissa in units of one thousand kilometres and ordinate is in km/sec.

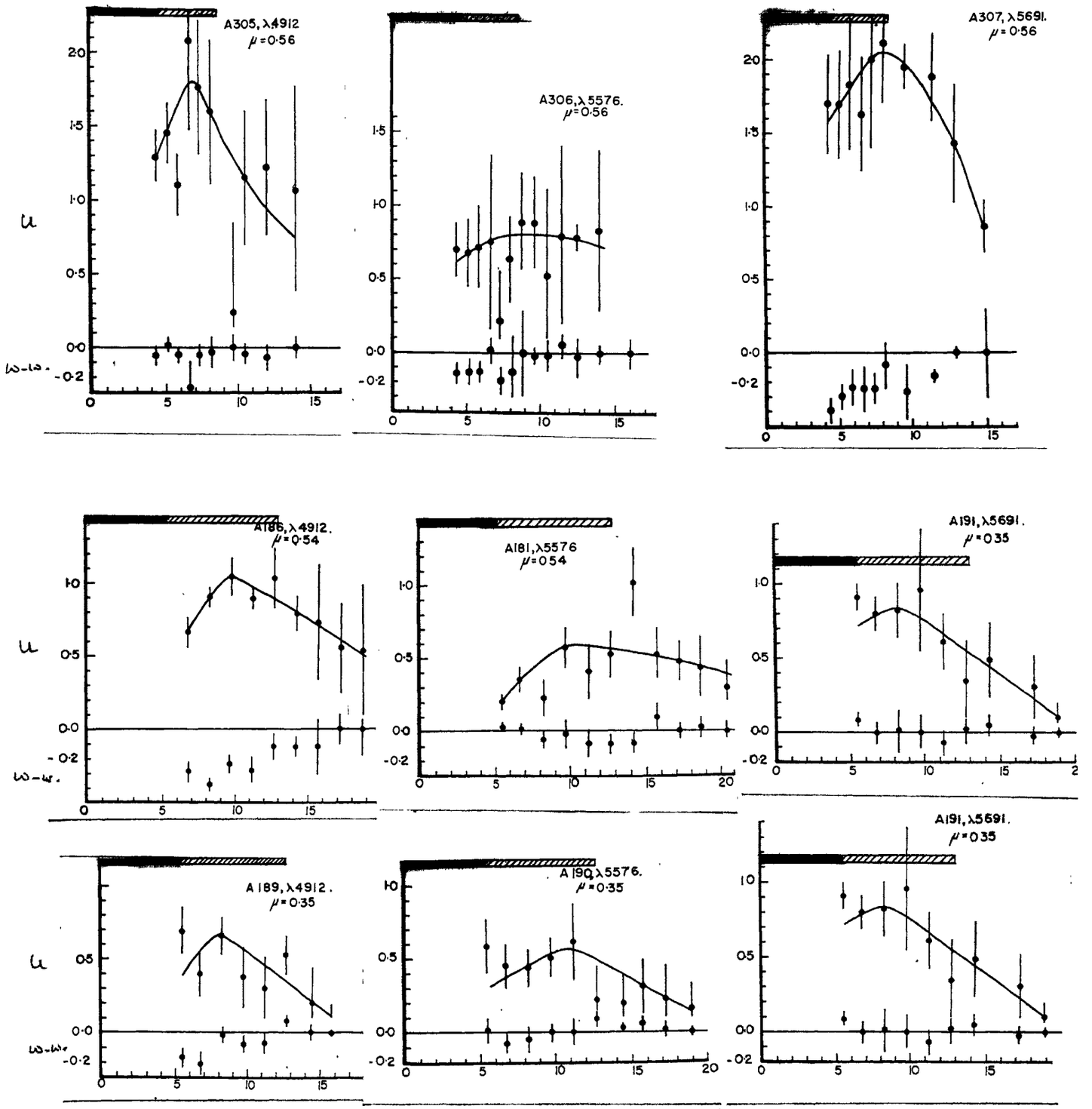

Figure III.5.- Radial and vertical velocity components, as a function of distance from the centre of the spot; abscissa is in units of one thousand kilometres and ordinate is in km/sec.

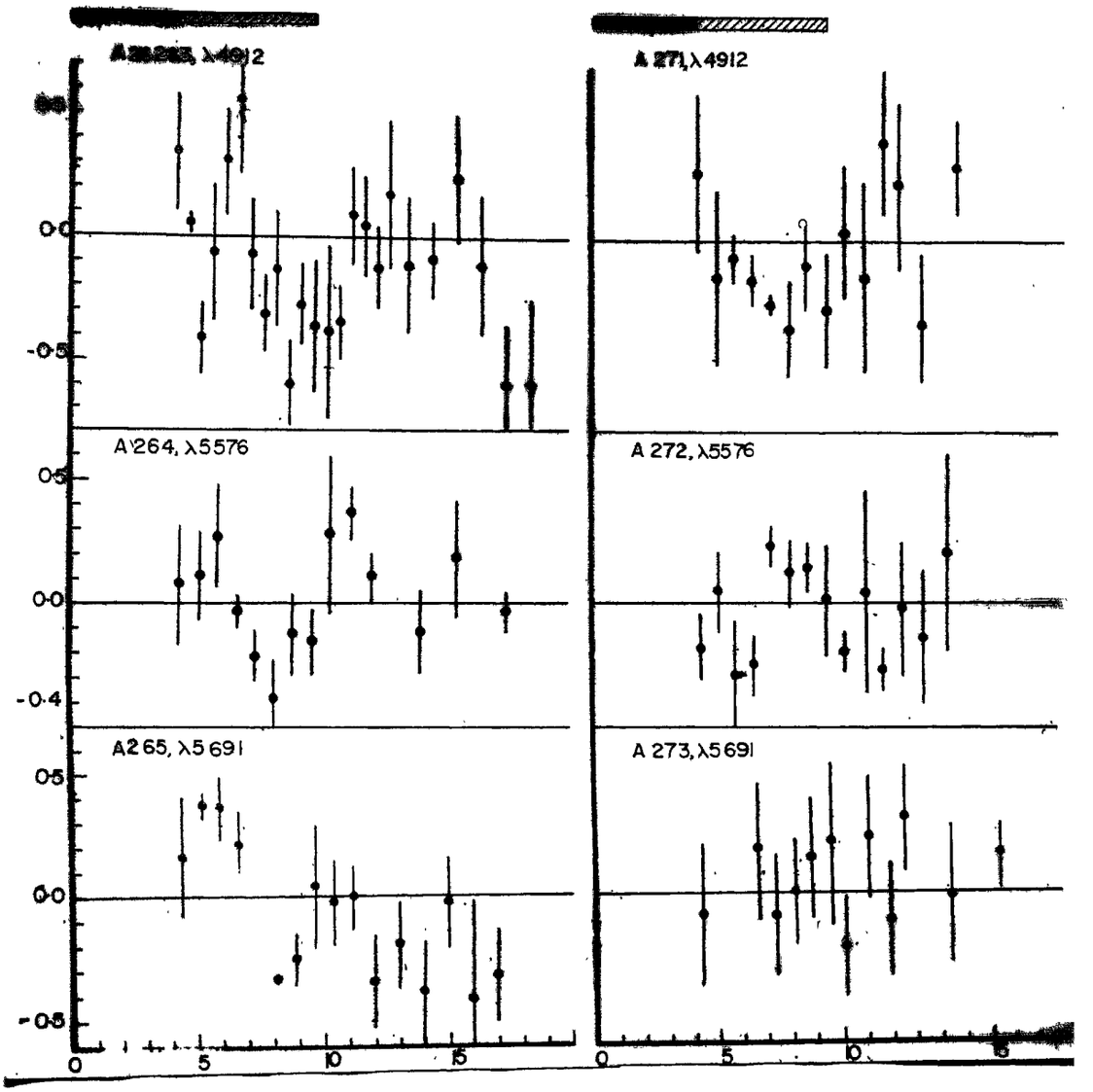

Figure III.6.- Tangential velocity as a function of distance from the centre of the spot; abscissa is in units of one thousand kilometres and ordinate is in km/sec.

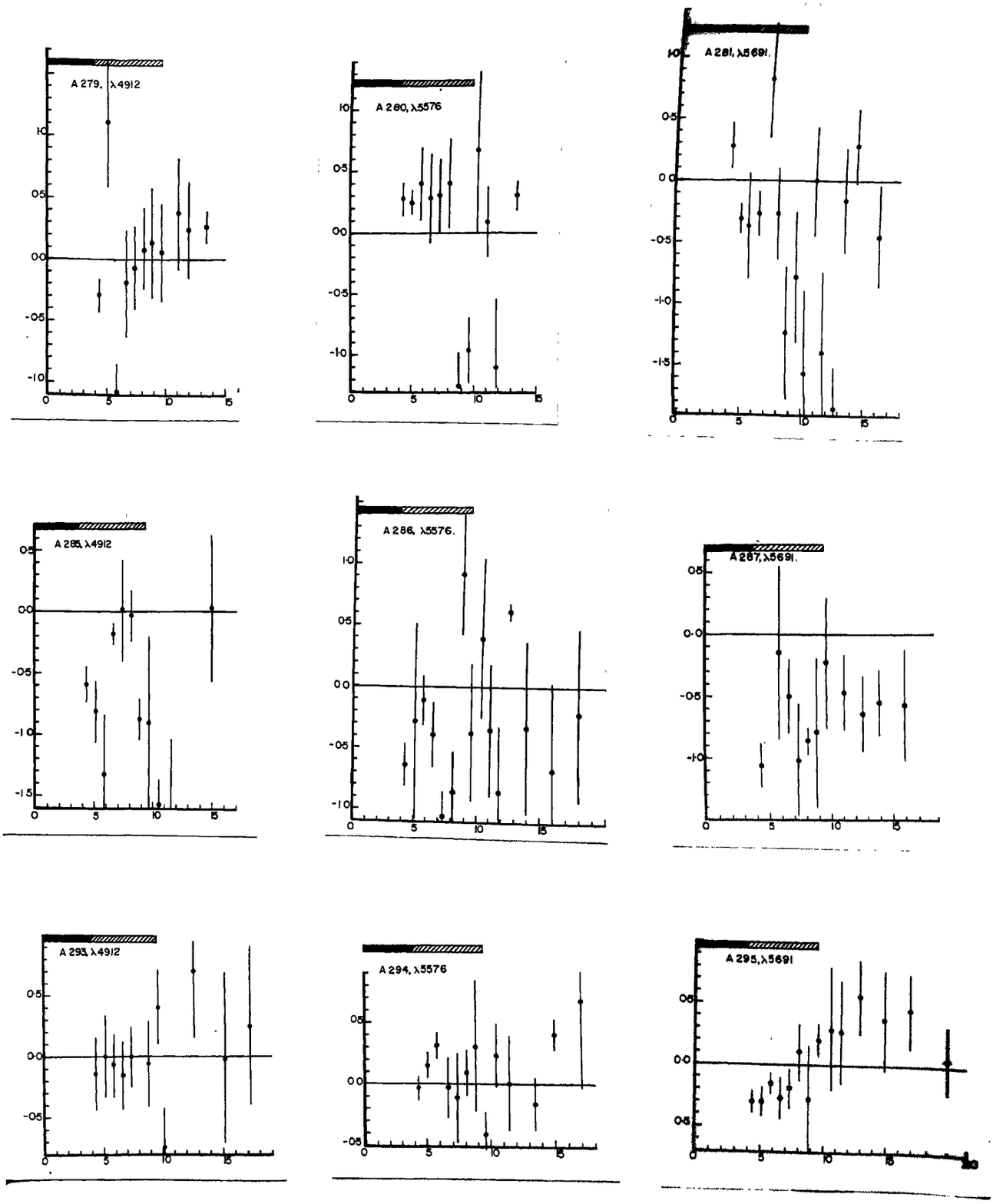

Figure III.7.- Tangential velocity as a function of distance from the centre of the spot; abscissa is in units of one thousand kilometres and ordinate is in km/sec.

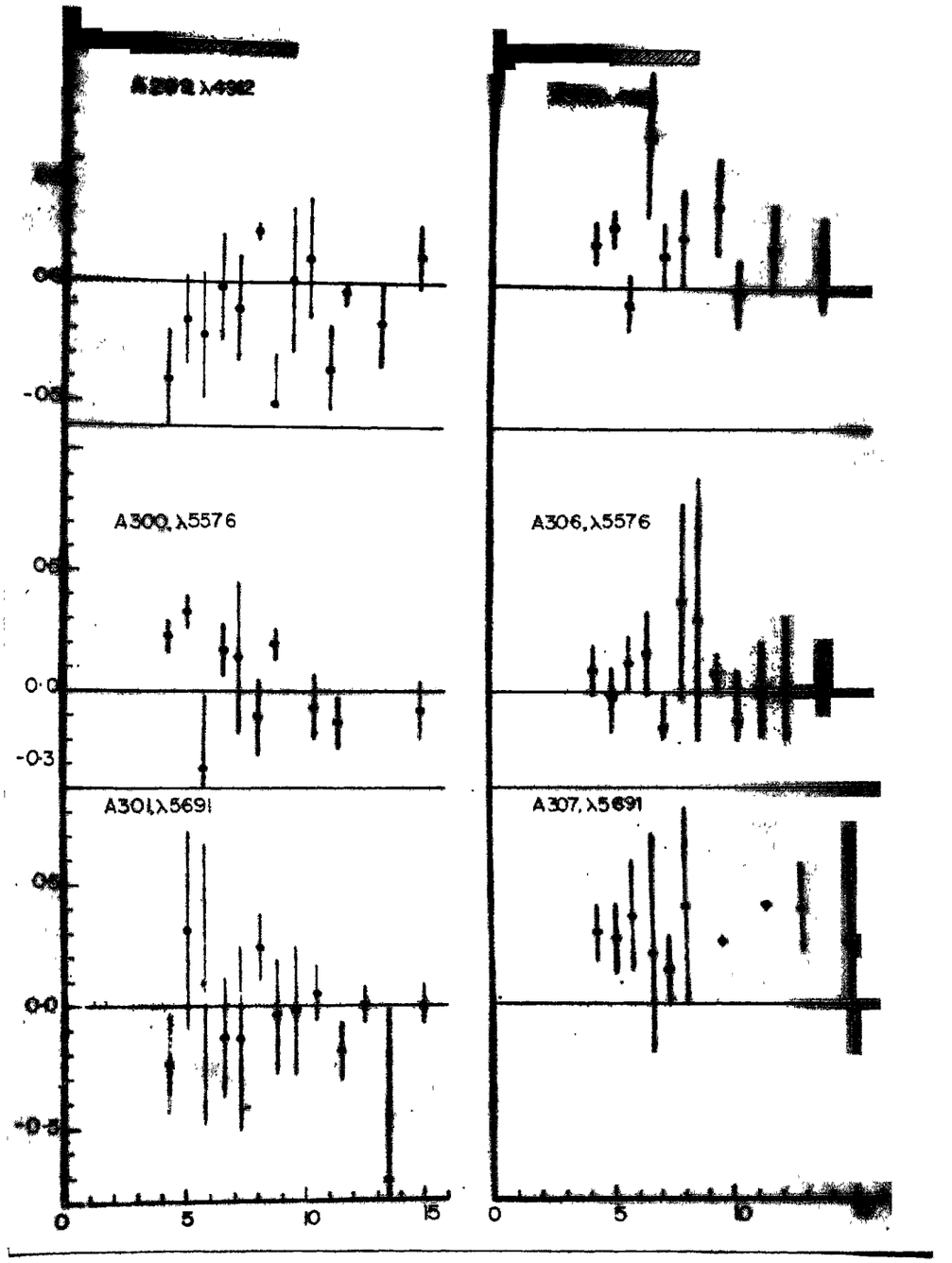

Figure III.8.- Tangential velocity as a function of distance from the centre of the spot; abscissa is in units of one thousand kilometres and ordinate is in km/sec.

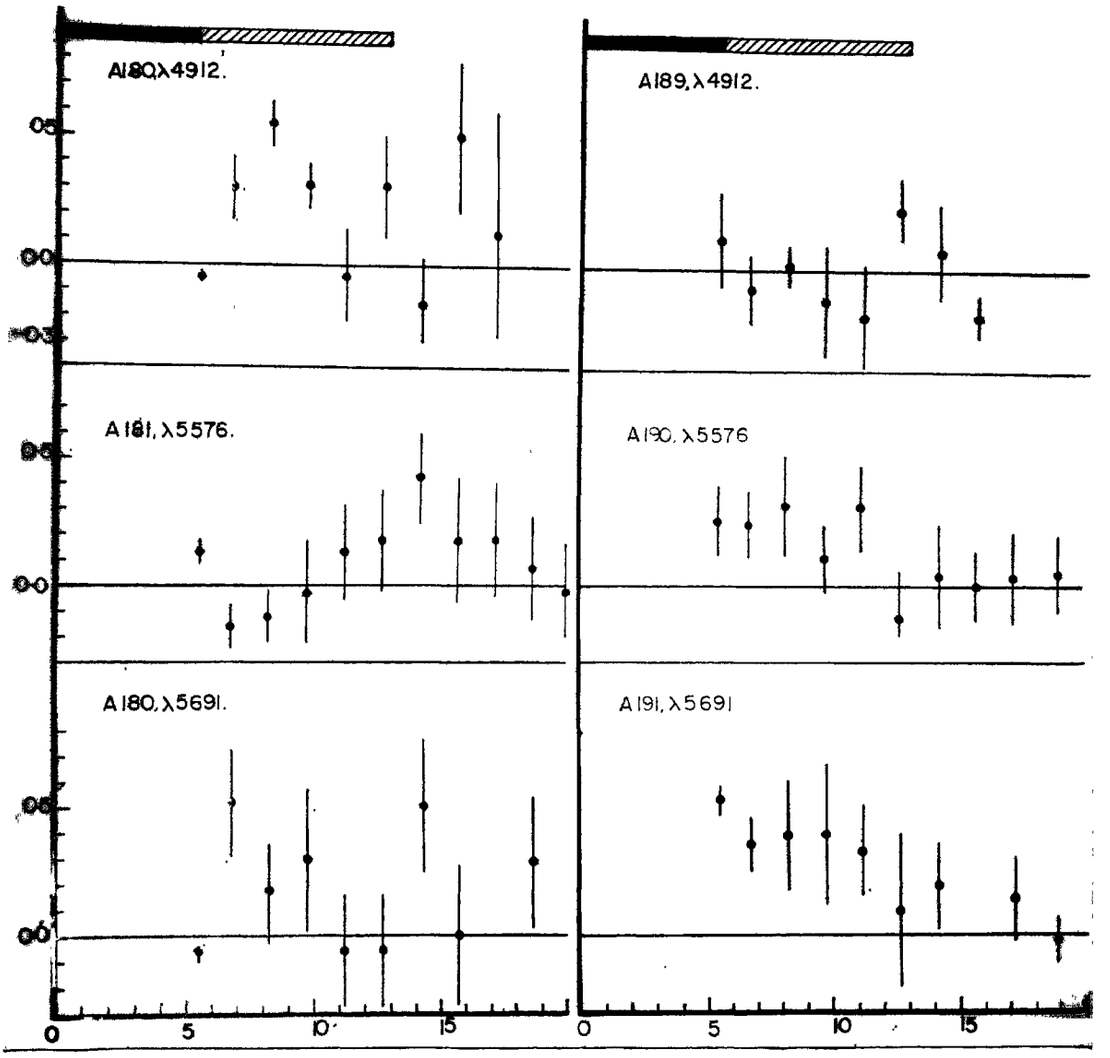

Figure III.9.- Tangential velocity as a function of distance from the centre of the spot; abscissa is in units of one thousand kilometres and ordinate is in km/sec.

The run of u and w components with distance from the spot centre can be seen in Figures III.3 through III.5. At the top of each figure, the approximate extents of the umbra and penumbra are represented by the dark and hatched regions respectively. These figures give the run of u and w components for each of the three Zeemaninsensitive lines 4912.027 A, 5576.101 A and 5691.508 A at nine disk positions of the spot, (μ= 0.35, 0.54, 0.56, 0.75, 0.86, 0.95, 0.94, 0.86, 0.74) observed on January 20, 21, February 9, 10,11,12,14,15 and 16 respectively. A quick glance of the run of radial velocity u, in Figures III.3 through III.5 shows that the radial velocity u, steeply increases, from near the umbral border, to attain its maximum value near the middle of the penumbral region. From its peak value the radial velocity gradually declines to become zero or nearly so far out in the photosphere. The rise to the peak value is always very steep compared to the decline of the radial velocity. The location of the peak radial velocity in the penumbra is not always at or near the middle of the penumbra. A slight shift in the location of the peak velocity across the penumbra could be understood as due to errors in locating the boundaries of the umbra and penumbra. Other important influencing factors, responsible for shifting the peak are scattered light and the definition of solar image.

If we compare the radial velocity curves at different disk positions of the spot, we notice immediateby considerable differences. The magnitudes of the maximum radial velocity (U_{max}), in all the three lines, show a decrease towards the limb, a conclusion that has also been obtained by Michard (1951) and

recently by Servajean (1961). Both these authors have interpreted this observation of decrease of the radial velocity towards the limb, as a manifestation of the phenomenon, that radial velocity (U_{max}) decreases with increasing height in the photosphere. However, the above conclusion that a decrease of U_{max} towards the limb, is an indication of the velocity variation with height, is subject to serious objection (Holmes 1963). Holmes has shown that the observed velocities in spots are affected by scattered light, in a way as to decrease the observed velocity. Further, she has shown that the influence of the scattered light increases rapidly when the observations are made close to the limb. The decrease in U_{max} towards the limb that we and other authors have observed, perhaps may not therefore be wholly due to the level difference in the photosphere. However, we have plotted the maximum radial velocity, U_{max} for each of the 3 lines, versus the disk position of the spot and is given in Figure III.10. It will be noticed from these curves that the slope of U_{max}: μ, for 5691.508 and 4912.027 A lines is almost the same, while for the stronger line 5576.101, the slope is different. The 5576.101 line of FeI (Rowland intensity 4) is formed at a higher level than either of the other two lines. The difference in the slopes between this line and the other two (Figure III.10) is probably due to the level differences in the formation of these two sets of lines in the solar atmosphere.

Comparing the pattern of radial velocity curves at different spot positions on the disk, we notice that the velocity pattern flattens out, for the positions near the limb. For spots located near the disk centre, radial velocity curves show a steep rise

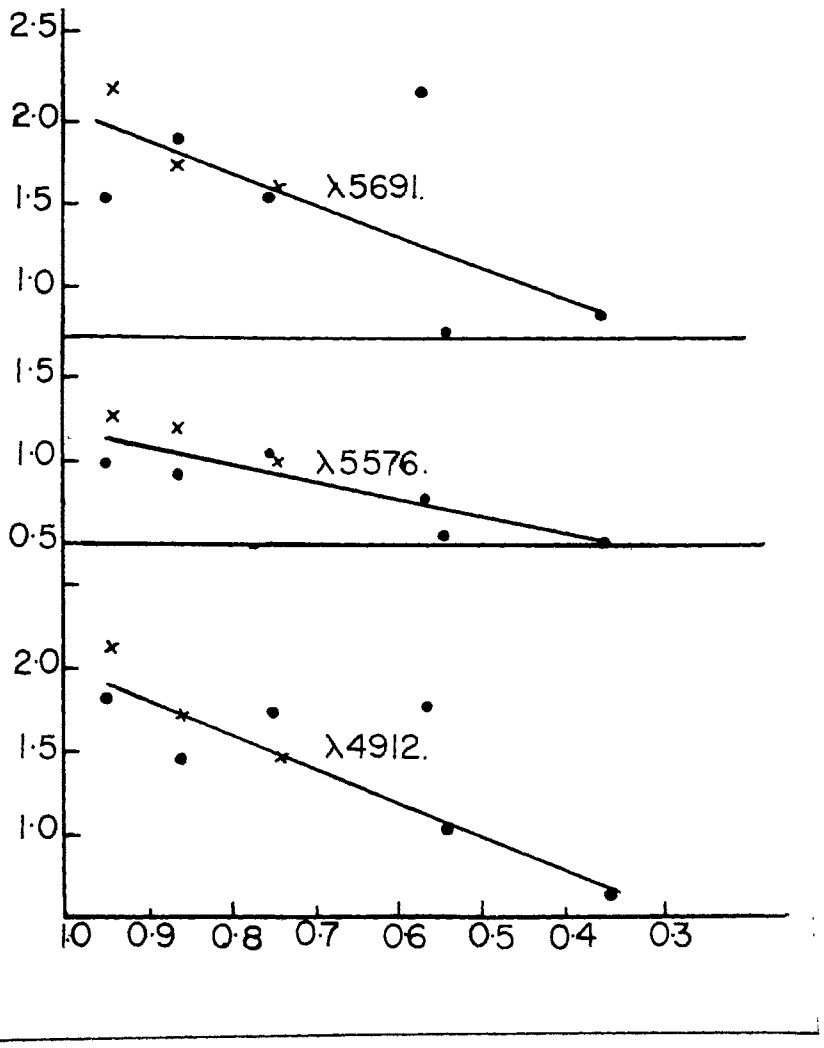

Figure III.10. - U_{max}: disk position of spot ( ) using 3 lines. × - East of C.M., • - West of C.M.

Abscissa: (cos) of spot
Ordinate: U_{max} in km/sec.

and relatively slow decline. The radial velocity run for all the three lines at one disk position appears to be very similar.

Considering the behaviour of the radial velocity pattern for each disk position, the slopes of the two halves of the velocity curves on February 9 ($\mu = 0.74$) appear nearly similar for all the three lines. On February 10 ($\mu = 0.86$), a very distinct hump, in addition to the peak velocity, developed near the outer edge of the penumbra. This hump in the velocity curve is visible in all the three lines. The position and the shape of the hump in 4912 A and 5691 A lines are very similar. In the case of 5576 A, the hump appears slightly detached from the main peak. It is difficult to assign any probable reason for an additional peak. A similar double peak in the radial velocity curve was also observed by Kinman (1953), in the case of Mount Wilson spot No.10955.

On February 11 ($\mu = 0.94$), the radial velocity curve became again single peaked, with a steep rise and fairly gradual fall. On February 12 ($\mu = 0.95$), the shape of the curve remained more or less the same. The peak velocity that had shown an increase on February 11, over the earlier days values decreased slightly. A decrease in U_{max} is noted systematically in all the 3 lines. Spectra taken on February 14 ($\mu = 0.85$) show fine details, because the seeing conditions during the exposures were exceedingly good. Fine penumbral details could be seen on all the plates. The radial velocity curves shown in Figure III.4, indicate large r.m.s. errors, and for a few points the radial velocities are large. However, the trend of velocity variation for all the three lines is similar with the earlier days results.

On February 15 (μ= 0.75), the slope and the position of U_{max} for 4912 A and 5691 A lines is almost the same. But in the case of 5576 A line the decline of the U_{max} with distance is very steep, and also the velocity peak occurs very near to the inner penumbral border.

Spectra taken on February 16 (μ = 0.56) and those taken on January 20 (μ= 0.54) were obtained nearly at the same spot positions on the disk. As mentioned earlier, the two series of spot spectra (KKL 12368 and 12375) refer to the same spot, and hence the velocity fields obtained on January 20 and February 16, can be compared for possible effects due to the age difference. For all the three lines, the U_{max} is systematically higher on February 16 compared to that on January 20. From these observations we infer that spots show larger velocities during their well developed phase, compared to the early phases. Servajean (1961) from the centre-limb variation of maximum radial velocity data, believes that U_{max} decreases with the age of the spot.

The variation of the maximum radial velocity with depth in spots was first suggested by Evershed (1910) and later a detailed investigation was made by St. John (1913). He observed from an analysis of the spot lines, that in the photospheric layers, the maximum radial velocity increases with increasing depth. With the aid of the theory of line formation and suitable model of the penumbra, it has become possible to determine the gradient of U_{max} with depth. In section 3.2 of this chapter, we have calculated the effective depths of formation of the two lines, 4912 A and 5691 A at five μ values (μ= 0.35, 0.55, 0.75, 0.85 and 0.95). Sunspot observations were made very close to these disk positions.

In Table III.3, we give the gradient of the maximum radial velocity with depth, at nine μ values. The mean gradient of U_{max} with height is about 4.0×10^{-3} km/sec. per kilometre in height, in the region 120-230 kms of photospheric depth. This value of the mean gradient of U_{max} is in agreement with that found by Servajean (1961) although Servajean had used the theory of line formation for faint lines and applied it to lines of Rowland intensity as high as 10.

Unfortunately, we cannot see deeper than approximately 300 km in the sunspot atmosphere. Actually, our measures of velocity field refer to only a thin layer of about 100 to 140 kms. Using some chromospheric lines such as the H-alpha and H and K lines of ionized calcium, it could have been possible to extend our measures to higher layers, over the spot. These measures are extremely difficult to make since the ionized calcium emission lines experience major changes in intensity and line width in the plage features over a sunspot.

3.5. Vertical velocity w

The vertical velocity w, is one of the three components obtained by using the method given in section 3.1, and is directed outwards normal to the solar surface. It will be recalled that while describing the method of solution of the equations of condition we assumed a constant coefficient of w, because it is independent of ϕ' (the position angle) and also since the sunspot surface is assumed to be plane. Our measures of vertical velocity are referred to the surrounding photosphere. Therefore, to

Table III.3

Gradient of U_{max} with depth at 9 disk positions.

Date	Mean μ position	Gradient of U_{max} in km/sec./km
Jan. 20	0.55	9.1×10^{-3}
Jan. 21	0.35	4.5×10^{-3}
Feb. 9	0.75	1.6×10^{-3}
Feb. 10	0.85	0.3×10^{-3}
Feb. 11	0.95	1.3×10^{-3}
Feb. 12	0.95	6.2×10^{-3}
Feb. 14	0.85	7.2×10^{-3}
Feb. 15	0.75	3.8×10^{-3}
Feb. 16	0.55	2.3×10^{-3}

Mean $\frac{du_{max}}{dh} = 4.0 \times 10^{-3}$ kms/sec./km.

obtain the component w, in the sunspot region, we have systematically tied the values of w, with a far removed point in the photosphere. The quantity $(w - w_o)$ and their r.m.s. errors are plotted in the lower halves of Figures III.3 to III.5.

From these figures, it will be seen that the direction of these small vertical velocities is systematically negative in the penumbra, the amplitude however is very small and is of the order of -0.3 km/sec and less. These velocities indicate decending motion in the penumbral region. The maximum values obtained by Servajean (1961) for the vertical velocities $(w - w_o)$ are of the order of -0.34 km/sec. He believes that this magnitude of the vertical velocities, directed inwards, is significant and in the penumbral region, the existence of the vertical velocities is very definite. Kinman (1952) also obtained small negative vertical velocities (-0.25 km/sec.) but he believes that those small velocities may be due to a systematic error in measurements. Our vertical velocity curves show $(w - w_o)$ velocities of small amplitude but are not systematic as those obtained by Servajean. The velocity variation in these cufves, with disk position, is very evident. A decrease towards the limb in the magnitude of $(w - w_o)$, is obsefved for all the three lines.

The magnitude of vertical velocity compared with the r.m.s. errors is small. However, the inclination (Adam 1963) of the magnetic lines of force to the vertical in the penumbral region suggests that a small vertical velocity component can be expected to occur, if the magnetic field has an influence on the motion of the sunspot material. This coupling between the magnetic field

and the velocity field is a logical possibility and hence we are justified in the conclusion that small scale vertical velocities exist in the penumbra.

3.6. Tangential velocity, v.

The existence or otherwise of the tangential component of velocity in sunspots, is yet to be confirmed. There are reliable and convincing observations in the literature that indicate the presence as well as absence of tangential velocities in sunspots. Evershed (1910, 1916) detected tangential components of the order of 0.25 to 0.35 km/sec. and even higher. Abetti (1932) analysed some 26 spots and found irregular tangential velocities of the order 0 to 5 km/sec., and suggested that the tangential motion varies from spot to spot. Calamai (1934) proposed a method for measuring systematic tangential components in spots. Using this method, he measured tangential components in 5 spots, and found that the trajectory of the material was of a logarithmic spiral type. The direction of the spiral, with respect to the vertical was sometimes clockwise or anticlockwise. In one spot he detected motion in both the directions. Kinman (1952) found from least square solutions of u, v and w in one spot, that the tangential component v was random in nature and was well within the errors of measurement. Although, at some locations in the spot, tangential velocities as high -0.5 ± 0.2 km/sec., were observed, Kinman believed that the magnitude of the tangential components was within the mean accidental error of the observations and hence, wholly spurious. In a later study of four spots Kinman (1953)

neglected completely the contribution due to tangential velocity. Servajean (1961) has also shown that the magnitude of v_t on most of the spot positions on the disk was very small. By comparing v with Δv, the departure from the assumption of the cylindrical symmetry of motion, he concluded that the magnitude of the tangential velocity was insignificant in the spot studied. From his Table III (Servajean 1961), sizable values of v (-0.33 to + 0.55 km/sec) occur on 27 and 30 April for spot positions at $\mu = 0.88$ and $\mu = 0.95$. From Servajean's results, the direction of the tangential velocities seems to change from one disk position to another.

We give our results of the tangential velocities and their r.m.s. errors in Figures III.6 to III.9. Tangential velocities in each of the several annular zones in sunspots are plotted for all the three lines used. The method for obtaining the tangential velocity v, is already described in section 3.1. In figure III.7, we notice almost no systematic variation of the tangential component v. Further, the r.m.s. errors are large compared to the amplitude of the velocity. If we consider only the tangential velocity curves for February 9 ($\mu = 0.75$), February 10 ($\mu = 0.85$), February 15 ($\mu = 0.75$), February 16 ($\mu = 0.56$) and for January 20 and 21 ($\mu = 0.54$ and 0.35 respectively), we notice slight systematic pattern of the velocity variation over and above the large r.m.s. errors. The maximum value of v is however, small and lies between 0.4 and 0.25 km/sec. The February 9 ($\mu = 0.75$), tangential velocity curves show a near simusoidal variation, about zero velocity, this behaviour is seen in all the three lines. On February 10 ($\mu = 0.86$) also a variation in v

can be seen. On February 11 ($\mu = 0.94$), February 12 ($\mu = 0.95$) and February 14 ($\mu = 0.86$) the tangential velocities show no systematic run and appear irregular. At a few points in the spot, the component velocity v, was found to be as high as 1.5 ± 0.6 km/sec. On these three disk positions of the spot, it is not possible to obtain any trend in the velocity run. On February 15 ($\mu = 0.75$) and February 16 ($\mu = 0.56$) the amplitudes of maximum tangential velocity show a decrease and a slight systematic trend in the velocity run. We do not find a one to one correspondence between the tangential velocity run for all the three lines. It will be too premature to assign this variation of v, as a depth effect, such as one found for the radial velocity component. On January 20 ($\mu = 0.54$) and January 21 ($\mu = 0.35$) the tangential velocity runs show a variation in amplitude along with the decrease in the maximum amplitude of v.

In all the tangential velocity variation curves, we notice large r.m.s. errors. These large r.m.s. errors could be due to the following reasons;

1. The number of points in each annular zone may be small.
2. Our basic assumption that the motion has a cylindrical symmetry about the centre of umbra, may not be wholly valid.
3. The number of unknowns (three u,v,w) are large, compared to the number of equations used in least square solutions.

Comparing our results with Kinman (1953) and Holmes (1961), we

notice that our velocities show larger r.m.s. errors. This in our opinion is due to the fact that we have taken three unknowns (u, v, w) in the equation of condition, while both Kinman and Holmes have neglected v, leaving the equations with only two unknowns.

From our observations of the tangential velocity and also on the basis of work briefly reviewed earlier, it will be realized that further observational corroboration is necessary before we can definitely recognize the contribution of the tangential component to the velocity field. Adam's (1963) recent measures of the orientation and inclination of magnetic field in spots, indicate the possibility of the presence of a tangential velocity. The high conductivity of solar material in sunspots, requires the motion to be along the magnetic lines of force. An interrelated study of the orientation of magnetic lines of force and the velocity field in the plane of the spot, could definitely enable us to verify the exitence of the tangential component. Adam's (1963) measures of the orientation and inclination of magnetic lines of force show that the azimuths of the magnetic vectors in spots, are not in agreement with the conventional supposition of a radial arrangement of the lines of force. Adam further notes that, while the field strength pattern remains stable, the direction of magnetic field varies from day to day.

As shown earlier, the largest contribution to the mass motion in spot penumbra comes from the radial component only. Nevertheless, the existence of the tangential motion has not been repudiated and on the other hand its presence may be in agreement

with the recent observations of Adam (1963). If we neglect the random character of the tangential velocity in our measures and only confine ourselves to the magnitude of the velocity, we have an argument in favour of its existence.

Adam's observations, show that the magnetic lines of force are not directed radially, but make certain angle with the radius vector of the spot. Considering the high conductivity of the solar material, the flow of material has to be along the magnetic lines of force. It would be impossible for the conducting material to 'slip-cross' perpendicularly the lines of force in a spot's magnetic field. With the existence of the azimuthal components of magnetic field, it implies that the motion should have a tangential component also. If on the other hand, we assume that the tangential velocity in spot penumbrae is zero or spurious and the motion is wholly radial, we are left with the only choice that the material partaking in the Evershed flow does not have sufficiently high conductivity for the 'freezing in' of the magnetic lines of force to occur. Therefore the material is not influenced by the magnetic field. The assumption that the sunspot material comprises wholly of low conductive material is highly improbable. If our observations show 'real' existence of the tangential velocities, with certain restrictions, then the problem of the flow of high conductive material in sunspots, conforms to a comprehensible picture. However, this conclusion is very tentative and should be considered with caution.

3.7. Determination of spatial magnetic field in sunspots.

We have determined the spatial distribution of the magnetic field in and around sunspots, for which we have measured spatial velocity fields. The aim was to investigate whether any inhomogenity in the magnetic field greater than 100 gauss caused any effect in the velocity field distribution. Along with this, the spatial magnetic field will also aid in studying the stability of spots.

We used the method first given by Hale for determining the magnetic field in spots. The two circularly polarized σ - components, produced by the longitudinal magnetic field, are changed into linear polarization by a quarter wave plate. The quarter wave plate used comprises of several 2 mm wide mica strips, joined edge to edge. The optic axes of the adjacent strips are perpendicular to each other. Behind this compound quarter wave plate, is placed a linear polarizer which suppresses one or the other of the two Zeeman components. In this way we obtain over the sunspot a 'Meander' pattern, produced by the compound quarter wave plate. Knowing the Zeeman separation $\Delta\lambda$, from the undisturbed line, one gets immediately the magnetic field in the spot, by using the formula;

$$\Delta\lambda = \pm 4.7 \times 10^{5} g \cdot \lambda^{2} \cdot H$$

where λ, wavelength of line in cms

g, the Lande's splitting factor

H in gauss

The Zeeman splitting for 6171 A line is 22,000 gauss per A and for 6303 A lines is 21,200 gauss per A.

We have made use of these two strongly Zeeman sensitive lines for the measurements of spatial magnetic fields in spots. The telescope and the spectrograph were the same as described earlier. For these measurements, the fourth order of the grating was used, where the dispersion of the spectrograph is about 6.0 mm per A. To cut off other orders we used a OG1 filter and Agfa Isopan 100, plates were used all through. Exposure times ranged from 35 to 45 seconds depending on the disk position of the spot. To determine the spatial magnetic field over the spots, we obtained five to six "Zeeman spectra", with the slit crossing the spot at a number of places. To know the orientation of the slit positions over the spot, we adopted the same technique of recording the spot and slit locations, as used for velocity measurements. We tied the polarity of the spots, with the visual measurement of Mount Wilson Observatory*.

Along each of the slit positions, we measured the Zeeman separation at intervals of 0.5 mm ($\approx$ 2".7 of arc) over the spot region. To facilitate measures, we used the spectrum projector and a measuring engine. This is the same projector as used for velocity measurements. In the case of magnetic field measures, we project the enlarged image (about 19 times) of the line to be measured on a stage attached to the measuring engine. On this stage, we have marked a fine line of about 1.0 cms long, this acts as a cross-wire for centering on the line, and also limiting 0.5 mm height of the spectrum to be measured.

---

* I am thankful to Dr. R. Howard for kindly supplying sunspot maps giving the magnetic field strength and polarity of some spots for comparison purposes.

With this arrangement, we determine the Zeeman separation in millimeters and then multiplying by a 'magnetic field factor', we directly get the magnetic field in gauss. The accuracy of this method is about 100 gauss. These values of magnetic field are shown in Figures III.11 and III.12. The spots observed and included in this study show a positive polarity that the magnetic lines of force are directed outwards from the solar surface. The number against each point on these sunspot maps, represents the magnetic field strength in units of 100 gauss.

The variation of magnetic field over a spot is well known from earlier measures. The maximum magnetic field exists near or at the centre of the umbra and decreases steeply on either side of it in the penumbral region. Around the middle of the penumbral region, the strength of the magnetic field decreases to a value half or less than half of the maximum value. For regular round spots the slope of the magnetic field is generally very steep. in the case of the spots, we have observed, the magnetic field becomes very small, probably less than 100 gauss or so, outside the outer penumbral boundary. Our method of measurement does not permit us to detect magnetic fields less than this order of magnitude. However, it is very unlikely that magnetic fields may abruptly cease near the penumbral boundary. Looking, at the 'Isogauss' maps, obtained by Crimean Observatory observers, it is clear that sizable magnetic fields exist, even beyond the visible boundaries of the spot.

Comparing the radial velocity field curves and magnetic field map, it is evident that the radial velocity increases in

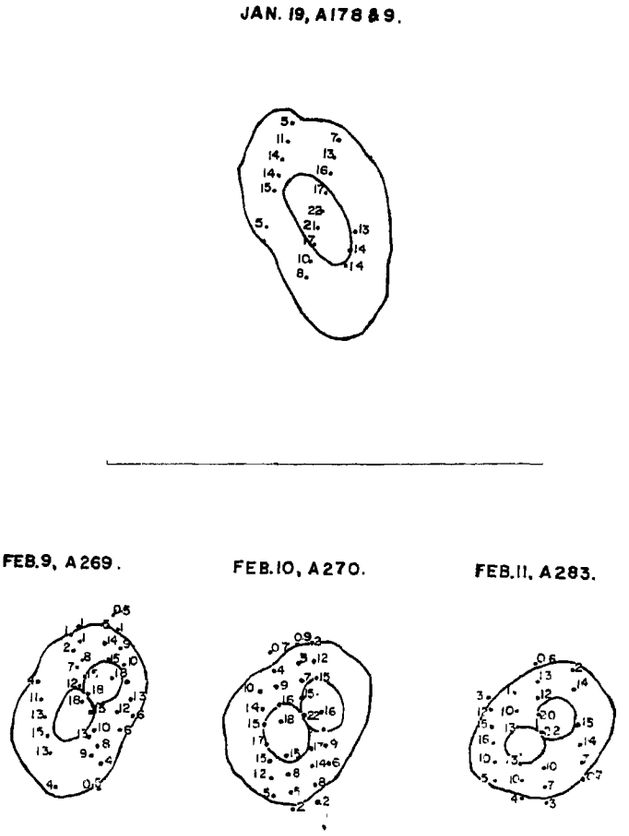

Figures III.11 and I.I.12.- Spatia
of 100 gauss.

the penumbra with increasing distance from the umbral border. The velocity attains its maximum value about half way between the umbra-penumbra boundary and the penumbra-photosphere boundary, and then gradually decreases to acquire zero or nearly zero velocity well outside the penumbral limit. The magnetic field however, decreases monotonically with increasing distance from the spot centre, to attain less than or equal to half its peak value near the middle of the penumbra.

It is well known that the convection in a conducting atmosphere, heated from below, is inhibited by the presence of magnetic field. In sunspot penumbrae also, the turbulent convection should be inhibited by the magnetic field. What we see in sunspots as the Evershed Effect, is the radial outward flow of material. Since the conductivity of solar material is very high, it is required that the lines of force will be 'frozen' in the material. This suggest that the magnetic field in the penumbra must be horizontal. Adam (1963) has shown that the inclination to the vertical of the lines of force becomes nearly 70° to 90° around half way in penumbra. Bumba (1960) has also shown that magnetic lines of force become nearly parallel to the horizontal near the outer penumbral boundary.

Recently, Danielson (1961) has shown from the pictures taken from stratosphere that long penumbral filaments are in fact elongated convection cells, called 'convection rolls'. The elongated appearance occurs due to the inclination of magnetic lines of force, to the gravity. He suggests that the long dimension of the convection cells is parallel to the horizontal component of the magnetic field. Similar to the granules, Danielson believes these

bright filaments to be hot "tubes of forces" rising upwards and the dark interspaces between the filaments are the cool "tubes of force" sinking down. Further he suggests that the 'convection rolls' due to the magnetic field are reinforced by the Evershed Effect.

In chapter V, we give a detailed analysis of some spectrograms showing fluctuations in the continuum intensity in the penumbral region, very similar to a fine granulation spectrum.

In this study of Evershed Effect and magnetic field, it was not possible to find, a point to point correspondence between the velocity and magnetic field pattern. However, magnetic field data are presented here in the hope that at a later date a possible correlation with the velocity field could be obtained.

CHAPTER IV

Asymmetry of lines in the penumbral region

4.1. The line asymmetry.

The important phenomenon of asymmetry of spectral lines in the sunspot penumbral region, was first discovered by Evershed (1916). He showed that near the outer boundary of a spot penumbra, the spectral lines develop a strong diffuse wing. The diffuse wing is always directed in the direction of Evershed displacement. A diffuse asymmetric wing in lines is easily seen on spot spectra taken by McMath et. al (1956). This asymmetric wing can easily be photographed with present day solar spectrographic techniques. In recent times, a detailed investigation of this phenomenon was made by Bumba (1960). Using a large solar image scale (5."9 of arc per mm) and a high dispersion, Bumba showed that a asymmetric wing develops near the outer boundary of the penumbra, and attains its maximum near the middle of the penumbral region. Further, he showed that under good seeing conditions and in favourable spot positions, the diffuse wing ('flag' in Bumba's terminology) can be resolved into a separate faint satellite. This line indicates Doppler shifts of the order of 5 km/sec or more. In a recent communication, Bumba (1963) has shown, that for favourable spot locations, the faint satellite line can be seen protruding into the umbra, where it attains its maximum separation from the parent line. Servajean (1961) has studied changes in the asymmetric nature of lines in spot regions and also at different spot locations on the solar disk. Holmes (1961) has also reported some measures of the asymmetric wings in spot spectra. McMath et. al (1956),

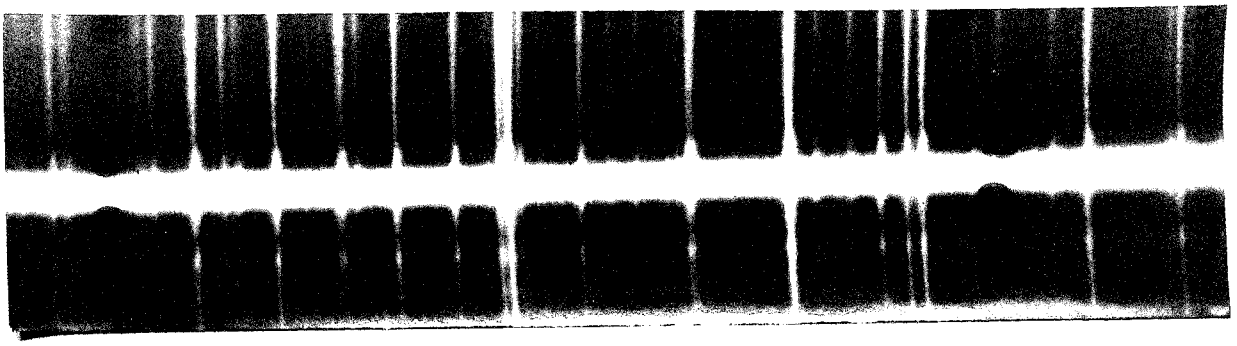

Figure IV.1.- Evershed's spot spectra taken on April 8, 1915, showing diffuse wing near the penumbral border.

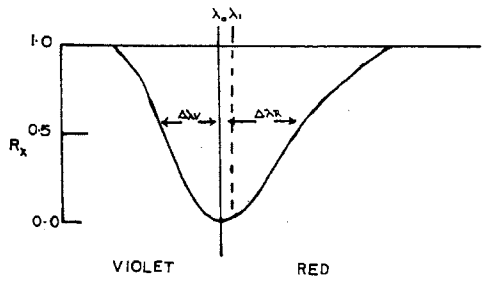

Figure IV.2.- The line asymmetry.

Servajean (1961) and Holmes (1961) have not reported the finding of a separate 'satellite' line as seen by Bumba (1961, 1963).

It is extremely remarkable for Evershed (1916) to have observed the diffuse wing in lines near the penumbral region, even though he had at his disposal a small solar image (40 mm) and relatively low spectrographic dispersion (about 0.9 A per mm). The very good seeing conditions prevalent on the occasions when Evershed obtained spectra at Kodaikanal, made responsible the discovery of the asymmetric wings. From some of the Evershed's spot spectra, in the Kodaikanal plate collection, we present in Figure 4.1 a positive showing clearly the diffuse wing, near the outer penumbral boundary. In this chapter, we present a detailed photometric study of this phenomenon. For a better understanding of this phenomenon, we must have high quality observations, made at various spot positions and in all types of spots.

We attempt to study quantitatively the variation of the asymmetry in lines, which we shall call henceforth as 'flag' (after Bumba).

1. over the spot region,
2. with the location of spot on the disk
3. at two portions of the line profile, and
4. with the strength of the line.

We shall use the term, "flag factor (F.F).", as a measure of the asymmetry in a line. We have defined the "Flag factor" (F.F) at any intensity value on a line profile as (Figure IV.2)

$$F.F = (\lambda_1 - \lambda_0)$$

where λ_0 is the wavelength of the central intensity point, and λ_1 is the wavelength of the centre of the line joining the equal intensity points on the profile.

We have measured F.F. at half intensity and at one tenth intensity points on the line profile. The purpose of measuring 'flag factor', at two places of the line profile is to see, how the asymmetry varies with depth in the line forming layers, since the wings of lines are formed effectively at a greater depth than the core.

To carryout these measures, we selected some of our finest spot spectra taken on three disk positions, namely on February 9 at $L - L_0 = 39^\circ.0E$, on February 12 at $L - L_0 = 0^\circ.0$ and on February 15, $L - L_0 = 39^\circ.0W$. All the three series of spot spectra were taken in three spectral regions (4912 A, 5576 A and 5691 A), with the slit crossing various positions on the spot. Details pertaining to these spectra are given in Table II.1. The slit positions over the spot are given in the velocity vector diagrams, presented in chapter II. All the spectrograms were calibrated with the aid of a Hilger six step wedge filter. The three selected series of spectrograms show fine photospheric details of the order of 1" of arc.

4.2. The photometric analysis.

For the photometric analysis, we selected only three slit positions on each of the spot spectra, taken on February 9, 12 and 15, and used three Zeeman insensitive lines (4912.027 A,

5576.101A, 5691.508A), except for spectra obtained on February 9. The approximate locations of the three slit positions over the spots are indicated in the Figures IV.3 through IV.5. We believe that these three slit positions for three disk positions of the spot, yield a picture that is very representative of the spatial aspect of the asymmetric wing in lines in spots. We obtained density traces, at several portions over the slit and parallel to the dispersion. The positions at which these scans were made are as follows:

1. at a point far removed from the spot,
2. very near to the penumbral border on either side of the spot,
3. near the outher boundary of the penumbra,
4. near the inner boundary of the penumbra.

In the case of slit positions crossing only the penumbra, four to five scans were obtained, in the region of the penumbra. For obtaining density traces, the microphotometer used was a Cambridge microphotometer modified to yield tracings on a recording potentiometer. The chart speed is adjusted to give a magnification of 25 times, the dispersion on the traces is thus 200 mm per A. A dial gauge capable of reading upto 10 microns was mounted in a direction perpendicular to the traverse of the microphotometer screw. This enabled us to determine the position on the plate in a direction perpendicular to the dispersion. For the precise knowledge of the scanned region on the solar disk, we used the wire shadows on the plate as the fiducial marks. The wire shadow was made to coincide very accurately parallel to the traverse of the

microphotometer screw. Dial gauge readings give directly the distance moved in the Y-direction from the wire shadow. We made use of the records of the spot and wire positions, made while photographing the spectrum, to exactly pinpoint the scanned position on the disk. In all these microphotometer scans, we used a scanning slit of about 0".8 of arc in height and about 0".3 of arc in width on the solar disk.

On 6 spectrograms, namely A262-3, 265, 285, 287, 299 and 301 and for one slit position, we have constructed intensity profiles of 4912.027 A and 5691.508 A lines. These intensity profiles are shown in Figure IV.6 as representative of some typical asymmetric line profiles. Along with this we have determined the 'flag factor' at one half and one tenth intensity points on the line profile, in the following manner;

Lines parallel to the dispersion at one half and at one tenth intensity points were drawn on the trace. Distances $\Delta\lambda_R$ and $\Delta\lambda_V$ (Figure IV.2) in the wavelength scale were read at one half and one tenth intensity values. $(\Delta\lambda_R - \Delta\lambda_V)$ thus gives the measure of asymmetry at $I_r/2$ and $I_r/10$, intensity values. In Figure IV.3 to IV.5, we give 'flag factor' along the length of slit, in all the three lines, and in three slit positions over the spot. The position of spot and slit is also drawn to indicate the approximate location of the slit orientation. Sight-line velocities measured along the length of the slit are also given. The positive values indicate flagging towards the long wavelength side while negative towards the short wavelength. The arrow indicates the direction of the centre of the solar disk.

Several inaccuracies are inherent in a photometric analysis of line profiles. They are chiefly due to;

1. the instrumental profile of the spectrograph,
2. the scanning slit may not be exactly perpendicular to the dispersion,
3. time constant of the recorder and amplifier, and
4. choice of the continuum.

The instrumental profile of our 18-metre Littrow Spectrograph, having a 200 x 135 mm size Babcock grating was determined using Iodine absorption lines with twice the 'normal' slit. The instrumental profile of this spectrograph is very narrow (less than 12 mA) and is very nearly symmetrical. In the fifth order, the theoretical resolving power of 600,000 is achieved. Iodine doublets near 5330 A, having an average separation of 9 mA, are clearly resolved in the fifth order. We have not corrected the intensity profiles for the small asymmetry due to the spectrograph, principally because, our measures of flagging are referred to the photospheric profile and the instrumental profile will not vary over small slit heights. Also, the small instrumental asymmetry can be neglected compared to the much larger asymmetry due to flagging.

We took great care in aligning the plate on the microphotometer carriage, and hence the error on this score is negligible. The combined time constant of the recording system is less than one second for a full scale deflection of the Brown recorder.

From the 'flag factor' plots in Figures IV.3 to IV.5 and the line profiles (Figures IV.6) we notice that the profiles in

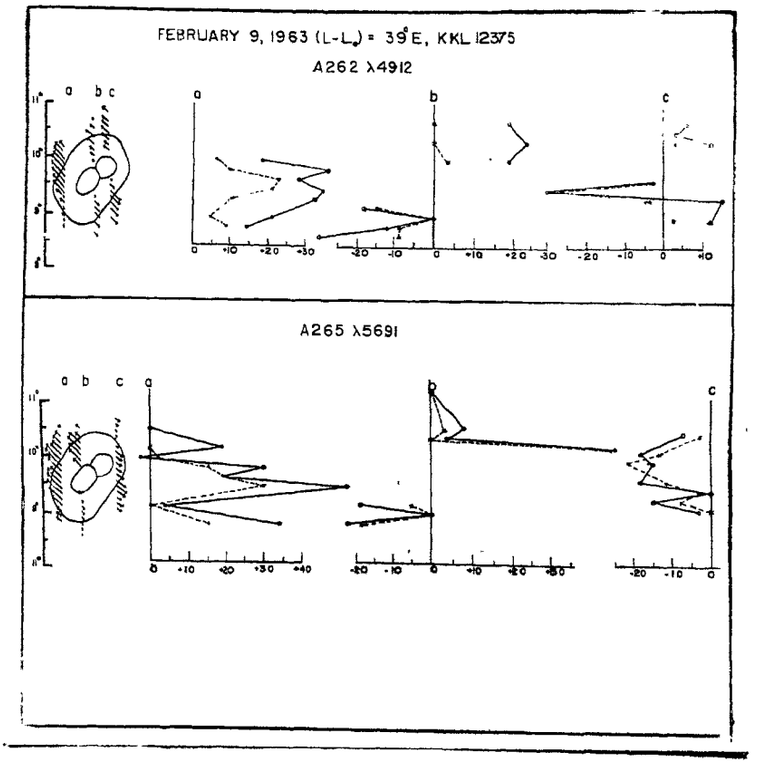

Figure IV.3.- Variation of flag factor over spot region.

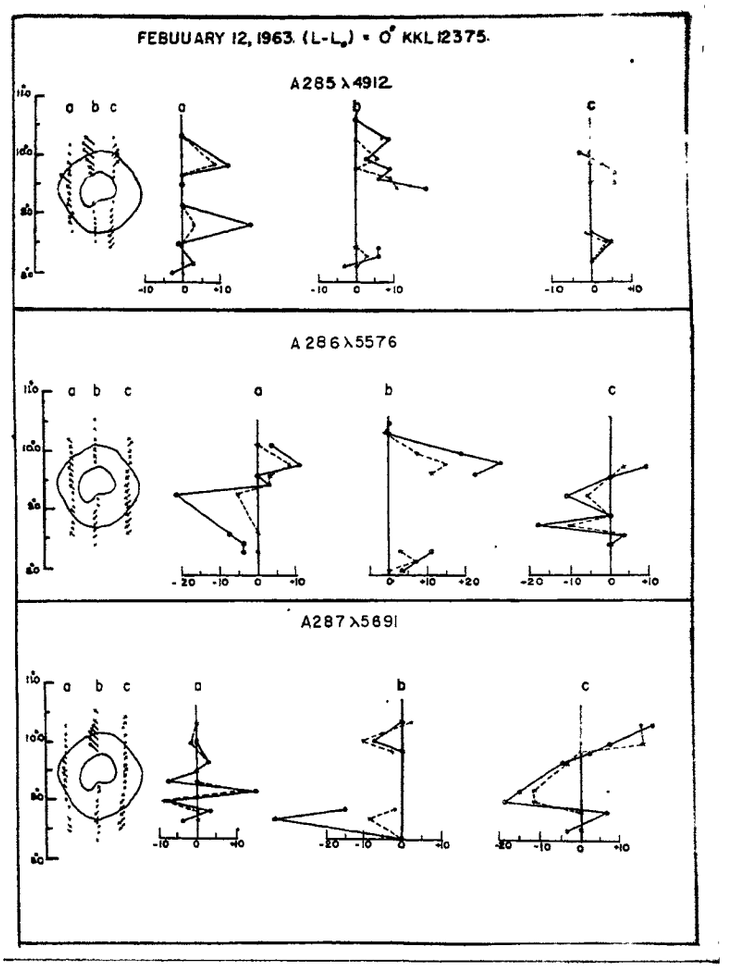

Figure IV(8) - Variation of flag factor over spot region.

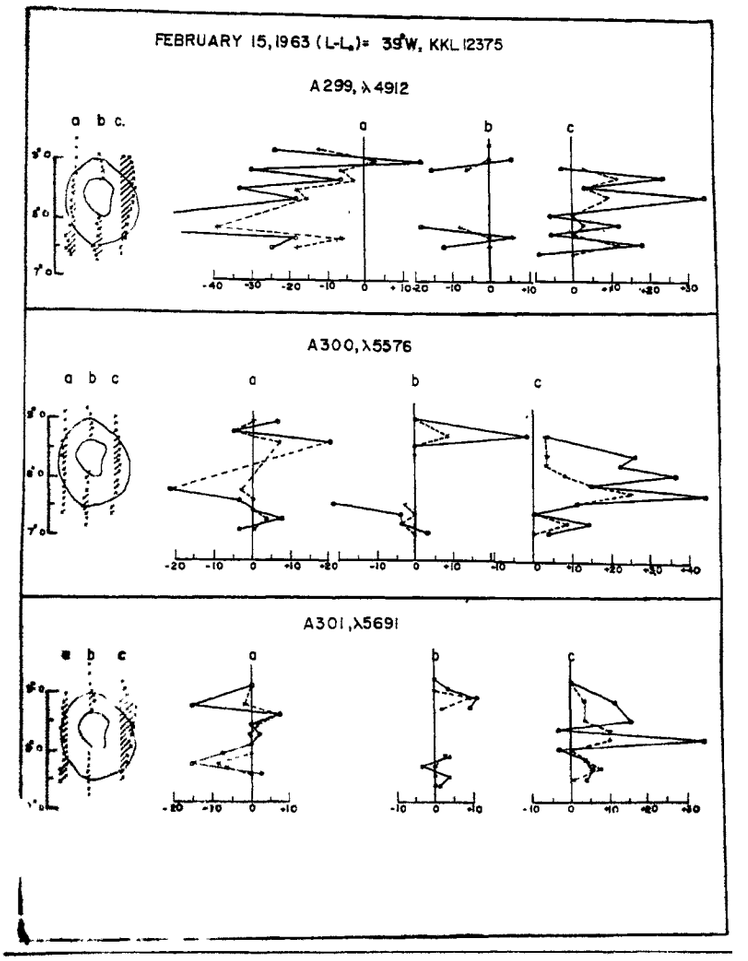

Figure V.5.- Variation of flag factor over spot region.

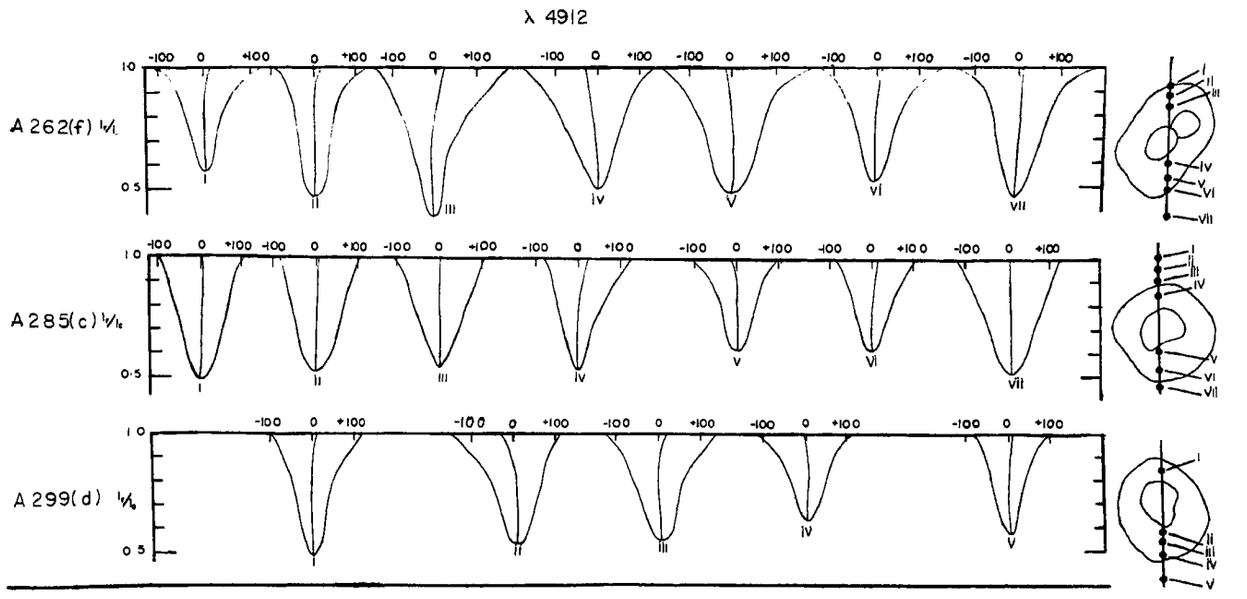

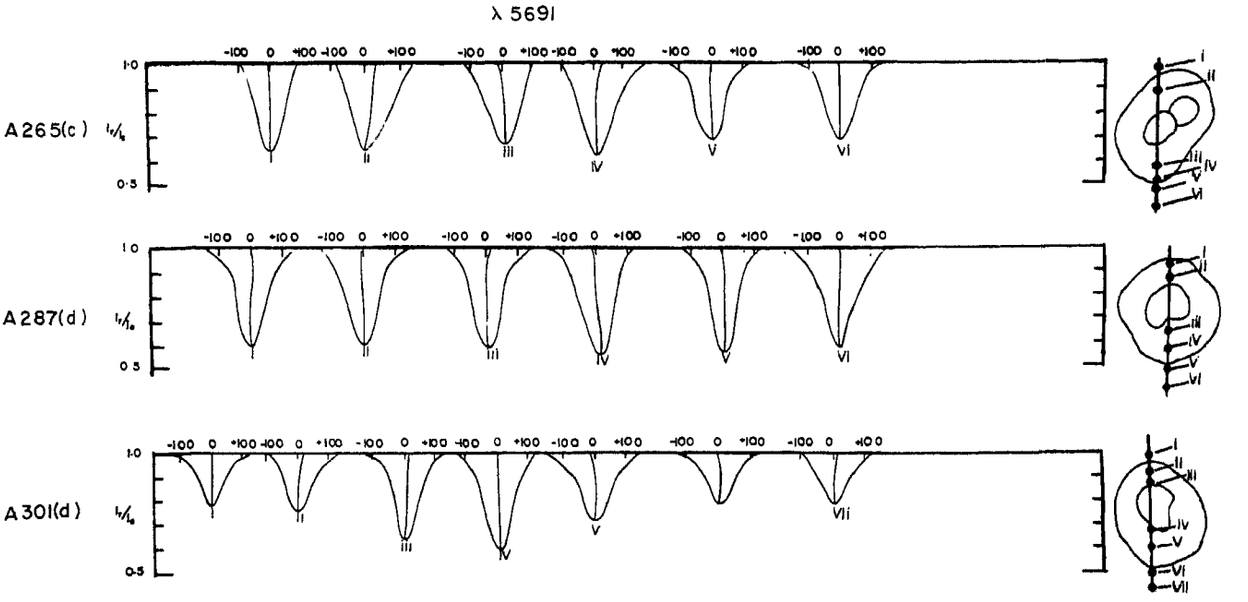

Figure V.6.- Line profiles over the spot, obtained in mA. Location of each of the line profiles is indicated in the drawings on the right.

the photosphere are symmetrical on all the three disk positions. Near the region very close to the penumbra, but outside the spot, the 'flag factor' for all the lines remain almost the same, as in the photosphere. In the region of the penumbra, they increase to attain maximum values around the middle of the penumbral regions. In the slit positions, other than the one crossing the umbra centrally, we find that the magnitude of the 'flag factor' fluctuates considerably. A line drawn joining the mid point of the line profile, Figure IV.6 shows clearly a steady increase in the asymmetry, towards the continuum. Also, the asymmetry follows the direction of the Evershed flow. This is true for all the three lines observed. In some spot regions, maximum asymmetry at 0.1_r of about 60 mA is noted. The maximum 'flag factor' is a function of the disk position of the spot. In the spot positions near the disk centre the value of maximum 'flag factor' is smaller compared to spots near the limb. Spot spectra obtained on February 9 and 15 at about 39^0 east and west of the central meridian, show larger asymmetry compared to those taken on February 12, near the central meridian.

A variation of the 'flag factor' is noted with line strength. A visual examination of some other spot spectra taken by Dr. M.K.V. Bappu at Kitt Peak National Observatory, Arizona, using a large solar image (35 inches in diameter) and with a spectrographic dispersion of 12 mm per A, show a decrease in flagging with increasing intensity of lines. The 4383 A and 4919 A lines of Rowland intensity 5 and 6_r show marked decrease in asymmetry. The direction of flagging in these strong and faint lines is same. An interesting feature in both strong and faint

lines is that the flagging does not extend in any case, beyond the penumbral limits. A visual examination of spot spectra taken in the 3934 A line of Ca^+, for a study of spatial distribution of the Evershed Effect in the chromosphere over the spot, show no such conspicuous flagging near the penumbral boundary. Moreeover, the calcium flocculi near this region makes the appearance of line asymmetry ambiguous. Bumba (1963) has shown that in $D_{1,2}$ lines of sodium, the flagging appears opposite to the Evershed shift. The direction of flag near the core of $D_{1,2}$ lines is opposite to that in the wings.

We have examined very carefully the spot spectra taken at Kodaikanal and at Kitt Peak Observatory by Dr. M.K.V. Bappu, for finding the 'satellite line', as reported by Bumba (1963, 1961). Both the series of spot spectra were obtained under good to very good seeing conditions. The image scale used at Kitt Peak was about 2".2 of arc and the spectrographic dispersion was 12 mm per A. Yet these plates do not show any indication of a satellite line in the umbral region. The flagging is very conspicuous in all slit positions over the spot region on these plates. Also, we have not found on any of these plates, the reported faint satellite line. The diffuse wing always appears to be joined with the parent line.

It is well known that the Evershed velocities become zero or very small, in the tangential slit positions. However, Bumba has observed conspicuous flagging in this slit position also. If this observation is verified in the future we shall have to interpret the phenomenon of flagging to be distinct from the

Evershed Effect. Further, it is well established by our observations and those made by Kinman, by Servajean and by Holmes, that the Evershed flow continues far into the photosphere. In no case, flagging has been observed to extend beyond the penumbral boundary.

Some of our spectrograms taken in very good seeing conditions, show flagging to occur more conspicuously in the darker regions of the penumbra. In the brighter regions the lines appear to be more or less symmetrical. Figure V.1 shows this appearance of the line under very good seeing conditions, in the penumbral region. The difference in the aspect of flagging under very good and average seeing conditions is apparent on plate A299 of February 15. Exposure b was made under average seeing conditions, while exposure f was obtained during moments of very good seeing. Figure IV.7 shows these two spectrograms. From Figure IV.7 it is apparent that in the darker (cooler) penumbral regions, the lines show considerable asymmetry, compared to the neighbouring brighter (hotter) region.

4.3. Development of a diffuse wing in lines in the photospheric regions.

A very similar phenomenon of diffuse asymmetric wings in lines, is noticed in the photospheric regions also. On our best spectra that show 'wiggles' due to granulation (less than 1" of arc details), one can see slight diffusion or 'flagging' in one of the wings of Fraunhofer lines. In the brighter photospheric regions, the lines appear very symmetrical and also slightly narrow. It is noticed that the diffuse wing develops invariably in the same direction as the Doppler displacement due to granular motion. We do not have at present any quantitative

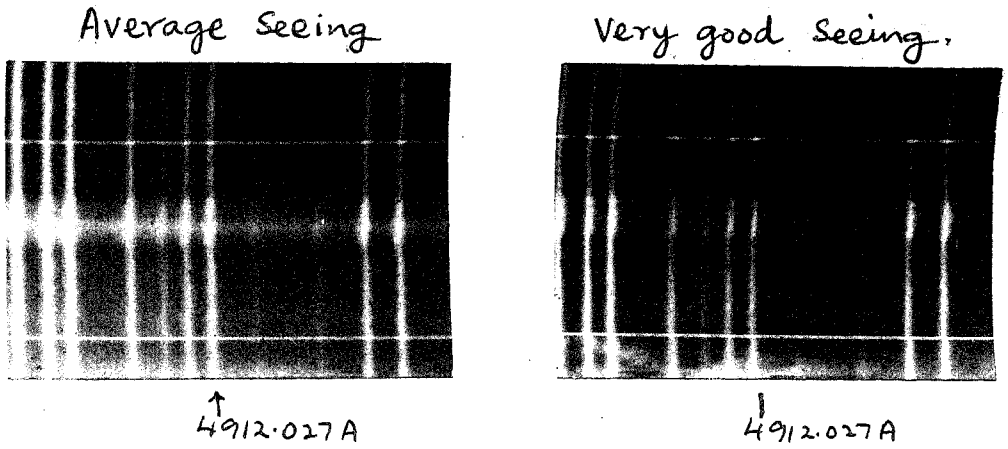

Figure IV.7.- Difference in penumbral details observed under very good (A299f) seeing conditions and under average (A299b) conditions.

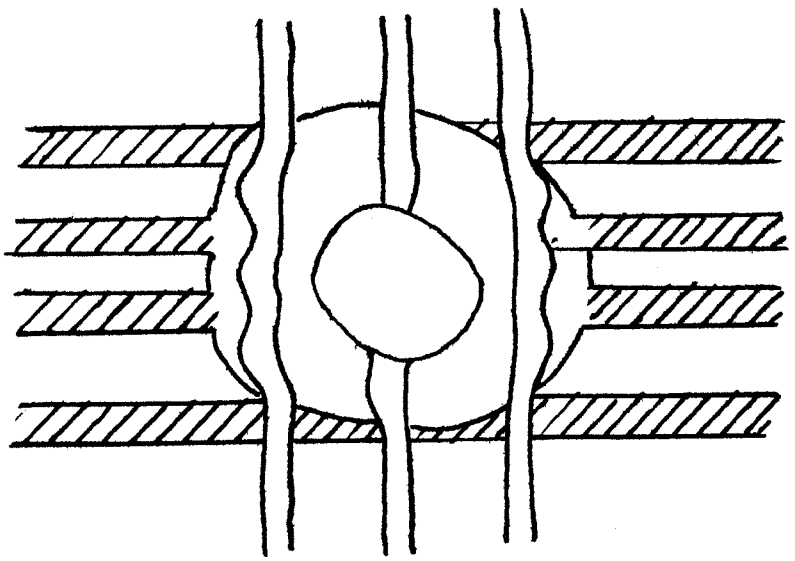

Figure V.1.- Drawing of the shape of spectral line over the spot, showing "flagging" in the dark interspaces in penumbral region.

estimate of the asymmetry of lines, in the photospheric dark regions. However, we are convinced that this phenomenon of 'diffuse wing' or 'flaring' of lines is real. A quantitative analysis of this phenomenon is required. Servajean (1961) has also reported the probable presence of a similar feature in granulation spectra.

4.4. Discussion.

The phenomenon of flagging in spectral lines in spots has been widely studied and its existence is fully confirmed. From the appearance of the line profiles and their variation in the spot and with spot's location on the disk, we find it necessary to postulate an association with velocity fields, either on the surface or deep in the sunspot atmosphere. Two plausible explanations have been put forward, one by Servajean and the other by Bumba. Servajean (1961) has suggested that asymmetry occurs due to the difference in velocities of different strata in a line forming layer. Bumba (1963) suggests, an upstreaming of material at the umbral-penumbral boundary, which bends to become horizontal in the penumbral region, and near the outer penumbral border the material turns downward again. The 'satellite' line that he claims to have observed, is due to the line of sight intersecting this layer of material flowing in the penumbral layer.

Our observations made under very good seeing conditions suggest, that the agency responsible for the asymmetry or flagging is more efficient in the darker (cooler) penumbral regions. The 'satellite' line referred by Bumba was not found on our plates, as well as, on Kitt Peak spectrograms. Perhaps, the appearance

of the faint satellite line depends on some other factors, such as, the contrast of emulsion and the right amount of exposure etc. However, until it is verified adequately we shall consider the satellite line to be non-existent.

As mentioned earlier, the asymmetry in lines is due to the effects of differential velocities in the line forming layers. This phenomenon is probably similar to the asymmetry in lines observed in shell stars. In the case of line-asymmetry in the penumbral region, the above process may probably be effective. The dimentions of the absorbing gas masses in the two cases are of course very different. Nevertheless, large line asymmetries could be observed, if the velocity between various 'strata' of the line forming regions is large. As noted earlier, the "flagging" is always directed towards the general Evershed flow. It therefore, seems that the motion responsible for the asymmetric aspect of lines is an additional relative motion superimposed on the Evershed flow. This relative movement in various layers responsible for the asymmetry in lines, attains its peak value near the middle of the penumbral region and ceases abruptly, at the outer boundary of the penumbra, while the Evershed flow continues well out into the photospheric region. Further, from the analysis of some of the very good quality spectra, we note that the processes responsible for the asymmetry are more efficient in the darker (cooler) interspaces, compared to the brighter regions in the penumbra.

To explain the increase of equivalent widths of lines in the dark granular interspaces, Edmonds (1962) and Teske (1963)

assumed an increase of microturbulence in these regions. The increase in asymmetry in the dark interspaces in penumbral region may probably be due to the added influence of microturbulence in these regions.

CHAPTER V.

Correlation between continuum brightness, equivalent width and sight-line velocity in penumbral region.

5.1. Continuum brightness variation.

It is well known that the variation in continuum brightness, over the length of a good solar spectrum, is due to the solar granulation. It is further established that the 'wiggles' in the Fraunhofer lines are due to Doppler displacements in the granulation spectrum. The early investigations of Richardson and Schwarzschild (1950) and of Plaskett (1954), have shown that material in the bright (hotter) solar granules is moving upwards, while the material in dark (cooler) intergranular spaces is moving inwards. Recently, investigations by Servajean (1961) and by Edmonds (1962) have shown that besides the variation in continuum brightness and in velocity, conspicuous variations in equivalent widths of the lines also occur over the length of the slit. Correlation studies by Servajean (1961) have revealed that dark elements show larger equivalent width, while bright regions experience a decrease in equivalent width. Edmonds (1962) has confirmed the findings of Servajean (1961).

During our investigation of spatial distribution of velocity fields over the spots, we noticed fluctuations in brightness and in width of lines, over the penumbral region of the spot spectrum. This is a phenomenon very similar to that seen on a granulation spectrum, though the cause for the brightness fluctuations in the two cases may be different. In this chapter, we present a study of a few spot penumbral spectra taken under very fine seeing

conditions, that show variations in continuum brightness as well as equivalent width of the lines.

Spot spectra obtained on February 9, 14 and 15 under very good seeing and transparency conditions for the study of spatial Evershed velocities in Kodaikanal spot No.12375, show clearly brightness fluctuations in the penumbral region. To the best of our knowledge such structure in the penumbra has not been detected spectroscopically earlier and hence these observations are the first spectroscopic ones that show up the brightness variation in the penumbral regions. For the study presented in this chapter, we have chosen the best among the three series of plates, that was taken on February 14, in the 4912 A spectral region. We obtained five spectra on the same plate A293, with the slit not at different positions on the spot. The positions of the slit over the spot are indicated in Figure 2.5 and are designated as b,c,d,e and f. Exposures b and f, crossing only the penumbra and exposure d crossing the umbra centrally, are used in this study. In Figure V.1, we give an approximate drawing of the appearance of the spectral line and the location of brightness fluctuation over the spot region. Reproductions of the three spectra (A293 b,d and f) are also given in Figure V.2. From these figures one can easily see a close correspondence between the dark regions in the penumbra and the widths of the lines. Superposed on these, are the usual velocity displacements due to Evershed flow. In Figure V.1, the hatched portions indicate the locationsof the bright streaks, seen on the spectra and the blank regions - the dark interspaces.

As mentioned earlier, a marked similarity exists between the fluctuations caused by granulation in the continuum brightness

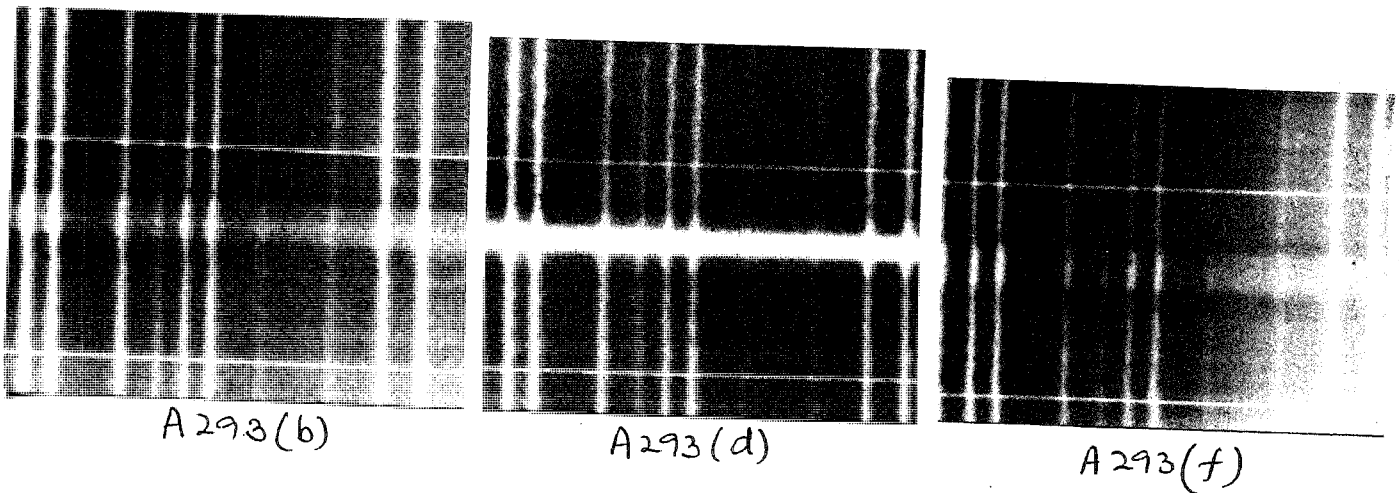

Figure V.2.- Spectra used for correlation study.

in the normal photosphere and the brightness fluctuations such as those observed by us, in the penumbral region. With this in view, we considered it of interest to investigate the correlation between the, 1. continuum brightness I and the equivalent width W, R(I-W), 2. equivalent width W and the sight-line velocity V, R(W-V), 3. sight-line velocity V and continuumbrightness I, R(V-I), in the penumbral region.

The brightness fluctuations in the continuum were determined in a region of the spectrum free from the absorption lines. The spectral region between 4913.6A and 4916.0A has only two very faint lines. Avoiding these faint lines, we made microphotometers scans, in the continuum, in a direction perpendicular to the dispersion. Microphotometer scans were obtained for all the three exposures (b, d and f), in the continuum regions. The scaning slit used was about 0".3 of arc wide and 0".6 of arc in height. The shadows of the two wires stretched over the slit, served as fiducial marks. We measured distance from one of these wire shadows to locate precisely the same place on the solar disk as on the spectrum. The density traces were then reduced to intensity values, using the characteristic curve obtained from the step wedge calibration spectrum. In Figures V.3 to V.4, we give the run of the continuum brightness variation for each of the three slit positions, over the spot. The ordinate is in arbitrary intensity units, small values of brightness corresponds to low intensity.

From these brightness fluctuation curves it will be seen

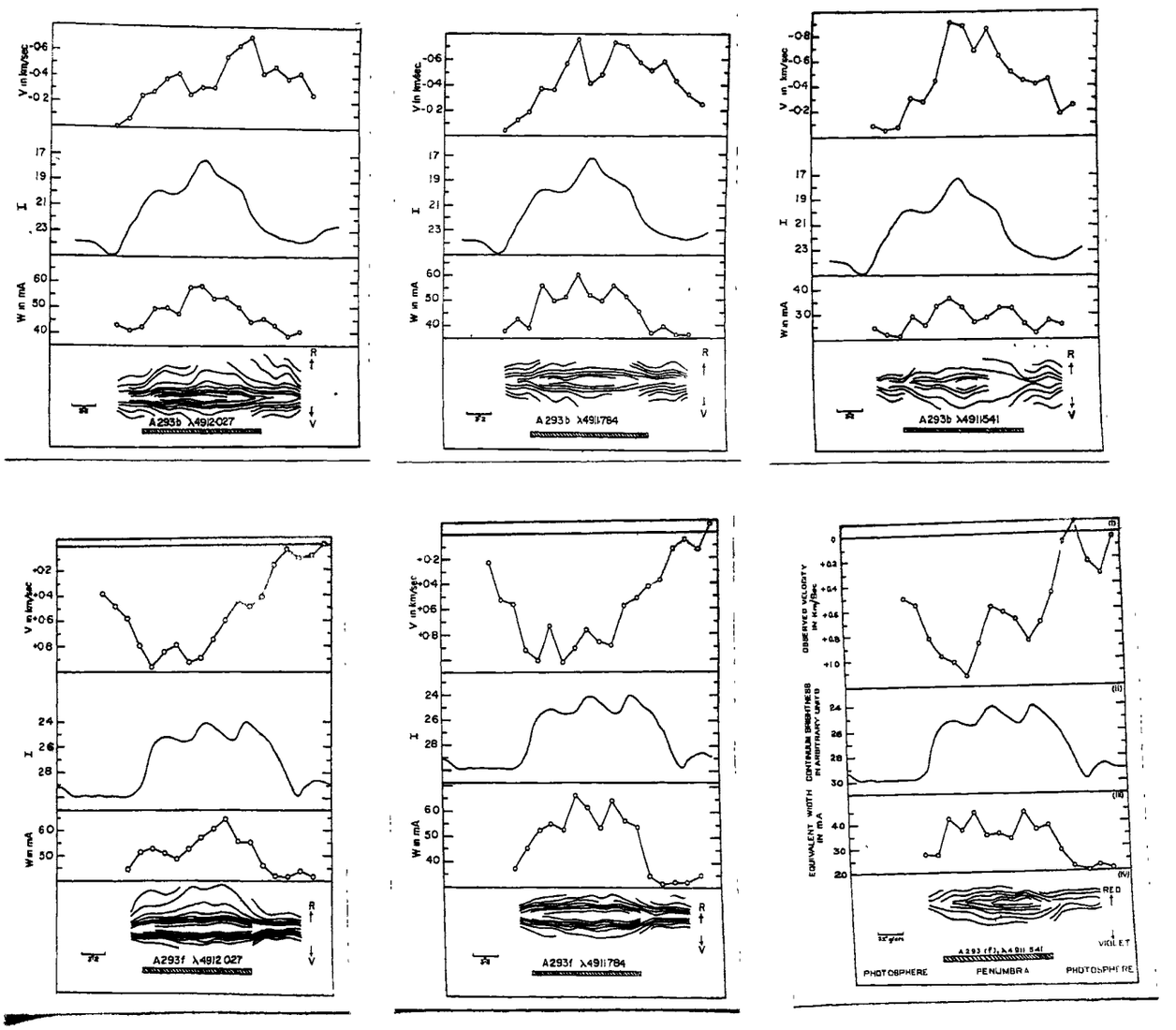

Figure V.3.- Plots of observed sight-line velocity V, continuum brightness I, in arbitrary units, equivalent width W, in mA. and the isophotal contour of lines over the spot.

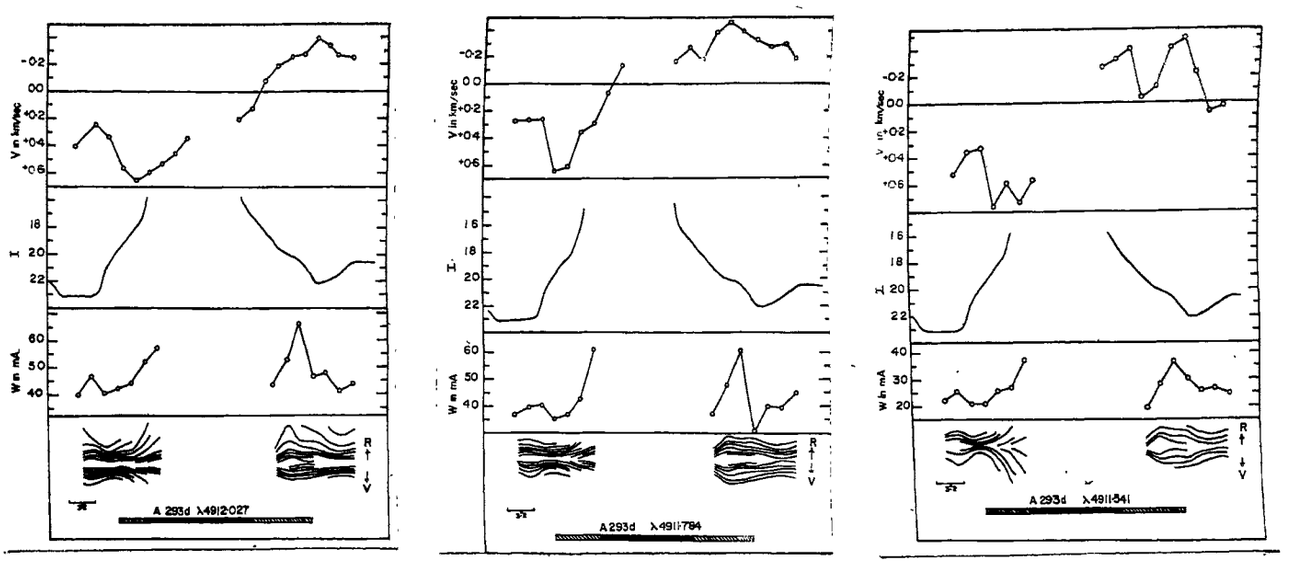

Figure V.4.- Plots of observed sight-line velocity V, continuum brightness I, in arbitrary units, equivalent width W, in mA and the isophotal contour of lines over the spot.

that a conspicuous variation in the continuum brightness occurs in the penumbral region. In the slit positions b and f, where the slit is placed crossing only the penumbral region, three distinct humps could be seen. Just outside the penumbral boundary, an increase in brightness compared to the photospheric brightness is very conspicuous. About 4 to 5 per cent increase in brightness occurs near the penumbral border. This increase in brightness is due to the bright ring around the penumbra. The 'bright ring' around sunspot penumbrae was observed spectroscopically by Das and Ramanathan (1953) and has been confirmed by many other workers. In most of our spectrograms, taken under good seeing conditions, a conspicuous brightening around spots could be seen. It appears that the brightening around spots is almost a permanent feature associated with every spot. The appearance of it perhaps depends on the definition of the solar image. In this study we are concerned with the continuum brightness fluctuations in the penumbral region only.

5.2. Equivalent width of lines.

The Fraunhofer lines show considerable variation in their width, over the region of the spot. To investigate the correlation between the width of lines and the continuum brightness variation, we measured equivalent widths at number of places over the spot region. Further, to see how the correlation between width and brightness varies with the line strength, we selected three lines. Table V.1 gives the details of these lines. The 4912.027 A line of Ni I is the Zeeman insensitive line, used for the velocity

TABLE V.1

Details of the chosen lines for this study.

Wavelength	Element	E.P volts	Rowland intensity	
			Disk	Spot
4912.027 A	Ni I	3.70	1	1
4911.784 A	Fe I	3.91	1	0
4911.581 A	Fe I	4.25	0	0

fields measurements. These three lines represent a small range in excitation potential and probably also a range in the effective depths of line formation. For the measurement of equivalent widths of lines, we obtained microphotometer scans parallel to the dispersion, at the same locations, where velocities were measured. The density traces were converted into intensity profiles. The area under the intensity profiles of lines were planimetered to give the equivalent widths of these three lines, at each of the scanned positions in the spot. The equivalent widths in milli Angstroms are plotted in Figure V.3 through V.4. A considerable variation in equivalent width of the line occurs in the penumbral region. The equivalent widths show an increase in the spot region compared to the photosphere.

For the three lines used in this study (4912.027 A, 4911.784 A, 4911.541 A), sight-line velocities in the sunspot were determined, using the method given chapter II. The run of the observed sight-line velocity is also given in Figures V.3 through V.4. These curves show marked fluctuations in the velocity field. The trend of the velocity variation follows the usual pattern of the velocity variation across the spot. Further, it will be noticed from these curves that the variations in the magnitude of velocity show a correspondence with the continuum brightness fluctuations. Isophotes of the three lines in all the three slit positions are also given in Figures V.3 through V.4. From Figures V.3 to V.4 giving the combined sight-line velocity, equivalent width and the continuum brightness variation for each of the three lines, one can notice a correspondence in the individual trends of variation. Keeping this in mind, we determined the correlation coefficients

TABLE V.2

Correlation coefficients between Brightness, Equivalent width and Velocity.

Wavelength	A293(b)	A293(d)	A293(f)
R (I-W): Correlation between continuum brightness and equivalent width.			
4912.027	-0.23	-0.64	-0.67
4911.784	-0.28	-0.35	-0.67
4911.541	-0.17	-0.41	-0.72
R (W-V): Correlation between equivalent width and sight-line velocity.			
4912.027	+0.87	+0.06	+0.44
4911.784	+0.55	-0.11	+0.77
4911.541	+0.30	-0.03	+0.83
R (V-I): Correlation between sight-line velocity and continuum brightness.			
4912.027	-0.13	+0.24	-0.47
4911.784	-0.20	+0.22	-0.49
4911.541	-0.26	+0.18	-0.43

R(I-W), R(W-V) and R(V-W), for all the 3 lines and for all the three slit positions, given in Table V.2.

5.3. The I-W correlation

The I-W correlation coefficients for each of the three lines from the sample obtained at the slit position b, show a systematic negative correlation. For the sample obtained from slit position f, the correlation is also negative, but the correlation is greater compared to that found in the sample from the slit position b. This latter slit position was nearer to the outer border of the penumbra, while the position f was very nearly in the middle of the penumbra. The difference in the magnitudes of the two correlation coefficients, can probably be accounted as being due to the slit position in the spot. However, the negative nature of the correlation is very certain and significant. This negative correlation implies that the darker (cooler) regions show large equivalent widths, while the brighter (hot) regions are characterized by smaller equivalent widths. This is a result similar to what one gets in the case of the photospheric granulation. Edmonds (1962) has examined the question of negative I-W cross correlation in the case of granulation. He believes that the processes reponsible for increasing the equivalent widths, by virtue of the changes in the population of the initial state of transition giving rise to a line, are not efficient enough to give a significant negative I-W correlation. He suggests in the case of the solar granulations, that the significant negative I-W cross-correlation should come from the increase of microturbulence in the dark regions of solar disk.

From the above observational data presented, it is now clear that considerable variations in continuum brightness and equivalent widths of lines occur in the penumbral region of sunspots. The I-W correlation analysis further shows that in the darker (cooler) penumbral regions, the equivalent widths show an increase compared to the neighbouring brighter regions. Before any plausible explanation for such variations in line widths and continuum brightness, can be given , we need at the outset a precise knowledge of the physical parameters, such as the temperature, pressure, conductivity and magnetic field, in the dark and bright regions of the penumbra. Similar to the case of solar granulation, two mechanisms proposed by Edmonds (1962) as responsible for the increase of equivalent widths may also be valid in the case of the penumbra. These are

1. an increase of microturbulence and
2. increase in the population of certain energy level in the darker regions.

To determine as to which of the two above processes are active in the penumbral region, we must have a better knowledge of the physical parameters than what we have today. The influence of magnetic fields which is very important in the penumbral region, compared to the general photosphere has to be taken into account, before the contribution due to microturbulence can be definitely assessed. Magnetic field inhomogeneities in the penumbral region could also be, to a certain extent, responsible for the variation of equivalent widths in the sunspot penumbra.

5.4. The V-V and V-I correlations. The sight-line velocities

that we have used here are the observed velocities over the spot. These values comprise both, the Evershed flow of material and the small scale fluctuations in velocity. For purposes of correlation coefficient determinations we have considered only the magnitudes of these velocities; the direction of motion is not considered. A fairly significant positive W-V correlation is obtained for the slit positions b and f. At the slit position d, when the slit crosses the umbra centrally, the correlation drops to small negative values. In this slit position the W-V correlation in insignificant. The V-I correlation shows negative values for the slit positions b and f, but for the slit position d, the V-I correlation is systematically positive. From these correlation coefficients involving V, it is difficult to arrive at any definite conclusion, as to whether the increase in velocity V, corresponds to an increase or a decrease in brightness I.

From the above discussion we observe that the relationship between the brightness and equivalent width fluctuations in the penumbral regions is similar to the relationship, between brightness and equivalent width in the normal photosphere.

REFERENCES

Abetti, G. 1932, Mem. Soc. Astr. Ital., 6, 353.

Adam, M.G. 1963, M.N., 126, 135.

Brekke, K., and Maltby, P. 1963, Ann. Astr. 26, 383.

Bhatnagar, A., and Punetha, L.M. 1963, Bull. Kodaikanal Obs. No. 162, 317.

Bruggencate, P. ten, Lust-Kulka, R., and Veight, H. 1955, Veroffentlichungen der Universitats-Sternwarte zu Gottingen, No.110.

Bumba, V. 1960, Izvestiya Krym. Astro. Obs., 23, 253.

Bumba, V. 1963, B.A.C., 14, 1937.

Calmi, G. 1934, Oss. Mem. Arcetri, 52, 39.

Chandrasekhar, S., and Breen, F. 1946, Ap.J., 104, 430.

Claas, W.J. 1951, Rech. Astr. Obs. Utrecht, 12, 1.

Danielson, R.E. 1961, Ap.J., 134, 289.

Das, A.K., and Ramanathan, A.S. 1953, Zs. f. Ap., 32, 91.

Evershed, J. 1909a, M.N., 69, 454.

Evershed, J. 1909b, Bull. Kodaikanal Obs., 2, No.15, 63.

Evershed, J. 1909c, Mem. Kodaikanal Obs., 1.

Evershed, J. 1909d, The Observatory, 32, 291.

Evershed, J. 1910, M.N., 70, 217.

Evershed, J. 1913, Bull. Kodaikanal Obs., 3, No.32, 17.

Evershed, J. 1916, Bull. Kodaikanal Obs., 3, No.51, 167.

Edmonds, F.N. 1962, Ap.J., 136, 507.

Hale, G.E., 1908, Ap.J., 28, 314.

Holmes, J. 1961, M.N., 122, 301.

Holmes, J. 1963, The Observatory, 86, 163.

Holmes, J. 1963, M.N., 126, 155.

Kinman, T.D. 1952, M.N., 112, 425.

Kinman, T.D. 1953, M.N., 113, 613.

Makita, M., and Morimoto, M. 1960, Pub. Astr. Soc. Japan, 12, 63.

Makita, M. 1963, Pub. Astr. Soc. Japan, 15, 145.

Mattig, W. 1958, Zs. f. Ap., 44, 280.

McMath, R.R., Mohler, O.C., Pierce, A.K., and Goldberg, L.1956, Ap.J., 124, 1.

Michard, R. 1951, Ann. Astr., 14, 101.

Michard, R. 1953, Ann. Astr., 16, 217.

Minkowski, R. 1942, Ap.J., 96, 306.

Minnaert, M. 1948, B.A.N., 10, No.339, 389.

Minnaert, M. 1953, The Sun, ed. Kuiper, 725.

Pecker, J.C. 1951, Ann. Astr., 14, 115.

Pierce, A.K., and Waddell, J.H. 1961, Mem. R.A.S., 68, 89.

Plaskett, H.H. 1952, M.N., 112, 414.

Plaskett, H.H. 1954, M.N., 114, 251.

Preliminary Photometric Catalogue of Fraunhofer lines, Rec. Ast. L' Obs. d'Utrecht, 1960.

Richardson, R.S., and Schwarzschild, M. 1950, Ap.J., 111, 351.

Schlesinger, F. 1899, Ap.J., 9, 159.

Schroter, E.H. 1963, Zs. f. Ap., 56, 183.

Servajean, R, 1961, Ann. Astr., 24, 1.

St. John, C.E. 1913, Ap.J., 37, 322.

Teske, R.G. 1963, Ap.J., 138, 271.

Walker, G.T. 1909, Bull. Kodaikanal Obs. 2, No.16, 71.

Wright, K.O. 1944, Ap.J., 99, 249.